Acta Pharmaceutica Sinica B 2026;16(3):1336−1367

Chinese Pharmaceutical Association
Institute of Materia Medica, Chinese Academy of Medical Sciences

Acta Pharmaceutica Sinica B

www.elsevier.com/locate/apsb
www.sciencedirect.com

REVIEW

Tuning mechanical softness as a design principle in drug delivery: A biomechanical perspective

Kangyuan Qi[a,†], Shasha Zhang[b,†], Xinying Bi[a], Zhiping Zhang[a,c,d,*], Conglian Yang[a,*]

[a]*Tongji School of Pharmacy, Huazhong University of Science and Technology, Wuhan 430030, China*
[b]*Wuhan Wuchang Hospital, Wuchang Hospital Affiliated to Wuhan University of Science and Technology, Wuhan 430030, China*
[c]*National Engineering Research Center for Nanomedicine, Huazhong University of Science and Technology, Wuhan 430030, China*
[d]*Hubei Engineering Research Centre for Novel Drug Delivery System, Huazhong University of Science and Technology, Wuhan 430030, China*

Received 30 April 2025; received in revised form 19 October 2025; accepted 29 October 2025

KEY WORDS

Drug delivery systems;
Flexibility;
Biomechanical design;
Mechanotransduction;
Therapeutic applications;
Tunable stiffness;
Biological barriers;
Mechanoimmunity

Abstract The *in vivo* performance of drug delivery systems (DDS) is profoundly dictated by their interactions with the biomechanical environment. Consequently, actively tuning the mechanical properties of DDS, such as softness and deformability, has emerged as an important design principle for enhancing their therapeutic efficacy. By intelligently adapting to the body's complex biomechanical system, these engineered DDS can orchestrate specific biological responses, such as enhanced tissue penetration, prolonged systemic circulation, and even regulated cellular signaling pathways through mechanotransduction. This review systematically explores, from a biomechanical perspective, how to optimize the behavior of DDS in the complex biological environments by actively designing their mechanical properties. We discuss how this principle was applied across diverse platforms, including coacervates, hydrogels, Pickering emulsions, extracellular vesicles, and liposomes, to achieve enhanced therapeutic behavior for treating challenging diseases like cancer, chronic wounds, and neurological disorders. By focusing on these tunable mechanical properties, this review aims to provide a theoretical framework and insights for the future development of DDS with improved adaptability and therapeutic efficacy in clinical settings.

*Corresponding authors.
E-mail addresses: zhipingzhang@mail.hust.edu.cn (Zhiping Zhang), conglianyang@hust.edu.cn (Conglian Yang).
[†]These authors made equal contributions to this work.
Peer review under the responsibility of Chinese Pharmaceutical Association and Institute of Materia Medica, Chinese Academy of Medical Sciences.

https://doi.org/10.1016/j.apsb.2025.11.037

1. Introduction

Biomechanical forces play an important role in various physiological activities within the body, including hair growth, cell proliferation, bone regeneration and cell migration[1]. Mechanical signals can be transduced into physiological or biochemical signals through mechanosensitive ion channels or receptors like PIEZO, G proteins-coupled receptors and adhesion proteins[2−4]. Since cells can sense and respond to mechanical stimuli, biomechanical forces play a pivotal role in regulating various physiological processes and influencing disease progression. For instance, tumor angiogenesis and liver fibrosis are significantly affected by changes in biomechanical forces, underscoring the need for targeted therapeutic strategies to regulate these behaviors[5]. Similarly, a key factor in T cell activation is the interaction between T cell receptor (TCR) and antigen peptide-bound major histocompatibility complex (pMHC), which is demonstrated to be involved in the biomechanical forces through a "catch bond" mechanism, highlighting the TCR's role as mechanosensor[6]. Moreover, macrophage phagocytosis is regulated by biomechanical forces, which involve a diffusion barrier formed by integrins and exclusion of CD45, a key step in phagocytosis initiation[7-10]. Overall, biomechanical forces are significant regulatory factors in various biological processes, affecting the life activities of organisms.

In recent years, some mechanically tuned drug delivery systems (DDS), characterized by tunable stiffness and deformability, have garnered significant attention for their ability to mimic the dynamic interactions within biological environments and then elicit the downstream mechanical signaling pathways. By fine-tuning physical properties such as stiffness and elasticity, researchers can customize the behavior of DDS *in vivo*, leading to improved therapeutic efficacy. Firstly, the inherent deformability of DDS enables distinct tissue penetration capacities and enhanced receptor−ligand interactions between the delivery systems and the cells. For instance, studies have shown that soft nanoparticles (NPs) could be deformed into spindle-shaped structures *in vivo,* for which the cumulative extravasation percentage was 5.7 times higher than that of spherical NPs in simulated pathological tumor tissues[11,12]. During T cell activation, the fluidity of DDS not only enhances the contact area between receptors in DDS and ligands on the cell surface, but also allows the flow behavior of receptors and ligands, thereby promoting the formation of immune synapses[13]. Secondly, cells can also directly sense the rigidity of DDS and regulate their *in vivo* processes, such as blood circulation and cellular uptake. Research has indicated that softer particles tend to circulate longer. Their deformability increases the energy required for macrophage endocytosis, resulting in sustained drug action while minimizing potential side effects[14]. Blood circulation of soft systems is also associated with their affinity for plasma proteins and immunoglobulins[15]. In terms of cellular uptake, although the research has not reached a consensus due to different elastic ranges of NPs used in the research and different cell types, the cellular uptake efficiency of DDS shows characteristics closely related to flexibility. As research in this field progresses, the potential of mechanically tuned DDS to revolutionize traditional drug delivery methods becomes increasingly evident, and DDS-related biomechanical forces play a pivotal role in regulating various physiological processes and influencing disease progression.

Although significant progress has been made in the current research on regulating the softness/hardness of drug delivery systems, few reviews focus on the field of DDS from the biomechanical perspective, and there is a lack of comprehensive analysis of the mechanisms by which flexibility affects the *in vivo* processes of DDS. Herein, this review from a biomechanical perspective, explores how to optimize the behavior of DDS in complex biological environments by actively designing their mechanical properties (Fig. 1). Unlike passively deformable DDS, mechanically tuned DDS are actively engineered to leverage biomechanical interactions, such as force-dependent cellular uptake, tissue penetration, and mechanotransduction, thereby representing a paradigm shift toward intelligent, context-responsive drug delivery. Firstly, the key mechanical parameters and characterization methods for assessing DDS flexibility are reviewed in this review to establish a biomechanical analysis framework. Then, we summarize the principle by which the mechanical properties of DDS affect the blood circulation, tissue penetration and cellular uptake, ultimately hoping to achieve the ideal therapeutic effect. Subsequently, through a series of case studies, this paper also offers a detailed implementation of this design principle in novel mechanically tuned DDS, such as coacervates, hydrogels, Pickering emulsions, extracellular vesicles (EVs), liposomes and other cutting-edge platforms. Finally, we summarize and discuss the current clinical application status and shortcomings of these DDS. In conclusion, by combining innovative drug formulation approaches with an understanding of mechanical signaling, DDS could significantly enhance treatment outcomes across a range of diseases, thereby pushing the frontiers of modern medicine forward. The ongoing exploration of these systems holds great promise for improving therapeutic efficacy and patient care in various medical fields.

2. Mechanical force as a design parameter: Key mechanical properties and characterization methods

2.1. Core mechanical properties for engineered drug delivery systems

Within the complex *in vivo* environment, DDS are subjected not only to chemical interactions but also to biomechanical forces, including fluid shear stress, tissue compression, and cellular traction. Traditional DDS design mostly focuses on parameters like size, charge, and surface chemistry, often treating mechanical properties as a passive, secondary outcome. However, a new design paradigm is emerging: one that transforms the mechanical flexibility of a DDS from a passive attribute into an actively engineered and precisely tunable core design parameter. This review is centered on this principle, wherein flexibility is conceptualized as a multidimensional feature, including intrinsic

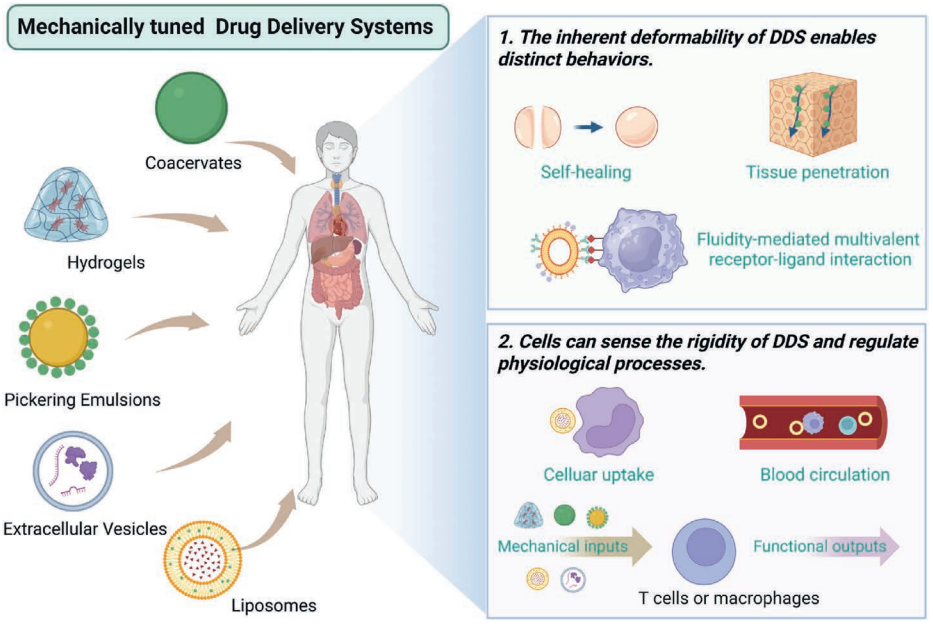

Figure 1 Schematic illustration of representative mechanically tuned DDS and their mechanisms of action, where mechanical flexibility is a key tunable parameter. These soft systems, including coacervates, hydrogels, Pickering emulsions, EVs, liposomes, and other platforms, play a crucial role in bioimaging, antitumor therapy, antiinflammatory treatment, and other disease interventions. Created in https://BioRender.com.

mechanical moduli (*e.g.*, elasticity and stiffness), structural deformability and interfacial characteristics, all of which can be evaluated by diverse techniques (Fig. 2). These special mechanical properties enable DDS perform well in processes such as cellular uptake, blood circulation, and receptor−ligand interactions.

2.1.1. Mechanical moduli

The mechanical moduli of DDS are mainly represented by Young's modulus, shear modulus, and bulk modulus[16]. Young's modulus is the most commonly used parameter for characterizing the stiffness of solid DDS, which is defined as the ratio between tensile stress and tensile strain, and thus serves as an index of a material's resistance to deformation. The higher the Young's modulus, the greater the stiffness of the NPs. The shear modulus is often used to characterize the rheological properties of DDS formulations (such as gels), and it is closely related to viscoelasticity, representing the ratio between shear stress and shear strain[16]. For viscoelastic materials, the shear modulus is usually expressed by the storage modulus (G') and the loss modulus (G''). The higher the G', the stronger the elastic properties of the material and the greater its ability to resist deformation. Higher G'' values indicate stronger viscous behavior and enhanced damping properties[17,18]. Bulk modulus is less frequently applied than Young's or shear modulus in routine DDS characterization, but it is relevant for understanding drug compressibility (especially polymorph stability), excipient behavior under pressure, and processes involving high-pressure treatments.

2.1.2. Structural deformability

Mechanically tuned DDS should have controllable structural deformability. After entering the organism, these DDS can undergo morphological changes (such as bending, stretching, and compression) to adapt to the biological environment, thereby achieving enhanced drug penetration, self-healing, and adaptability to irregular wounds. This deformation does not cause the rupture or damage of DDS[11]. However, it should be noted that deformability is often confused with stiffness. In fact, the concepts of the two are not the same. Stiffness measures the ability of a system to resist deformation. The greater the stiffness, the harder the material is and the less likely it is to be stretched, compressed or bent. Deformability measures the ability of DDS to withstand deformation without being damaged. The greater the deformability, the softer or more resilient the material is, and the greater the amount of deformation it can withstand.

2.1.3. Interfacial characteristics

The interfacial characteristics of DDS include aspects such as surface tension and interface adhesion energy, which determine how DDS interacts with biological interfaces and deforms when in contact. Generally speaking, the interfacial tension of DDS, such as liposomes, stems from the hydrophobicity of the lipid tail[19]. The surface tension of DDS is a key factor influencing its flexibility. Low surface tension means that DDS are softer and more prone to deformation when subjected to external forces. The method of regulating flexibility by reducing surface tension has been widely used. As another key feature of the interfacial characteristics, the interface adhesion of DDS is reflected in two aspects: microscopic adhesion and macroscopic adhesion. Microscopic adhesion refers to the deformation of soft NPs when they come into contact with the cell membrane and adhere to it. This adhesion to cells can achieve long-term receptor activation, thereby achieving the effect of immunotherapy[20-22]. Macroscopic adhesion includes the adhesion of hydrogels to the surface of wounds, which can promote wound healing through their viscoelasticity[23].

2.2. Mechanical properties as a design parameter

The transition of mechanical flexibility from a passive attribute to an actively engineered design parameter is central to modern DDS

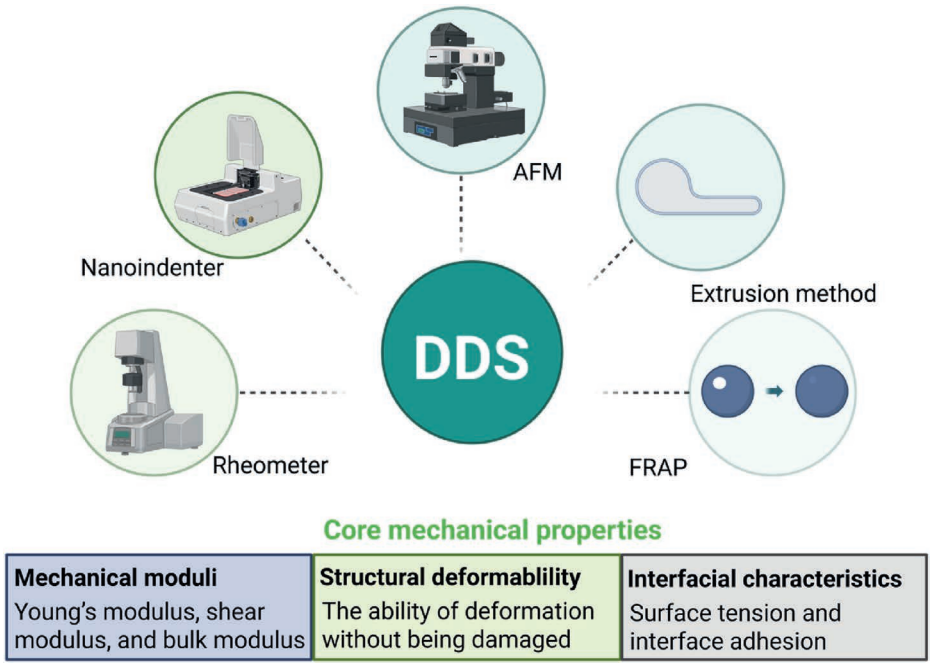

Figure 2 Key mechanical properties and characterization methods for mechanically tuned DDS. Created in https://BioRender.com.

development. This requires a precise understanding and quantification of key mechanical properties, which can be broadly categorized into mechanical moduli (*e.g.*, Young's modulus), structural deformability, and interfacial characteristics (*e.g.*, membrane fluidity and adhesion).

Quantifying these properties necessitates a multi-modal approach, as no single technique can capture the full spectrum of a DDS's mechanical behavior in a complex biological environment. Techniques such as Atomic Force Microscopy (AFM) and nanoindentation are important for probing the stiffness of individual nanoparticles at the nanoscale. However, interpreting these measurements requires careful consideration of potential artifacts, such as the substrate's "bottom effect", especially for ultra-soft materials. For assessing bulk properties and viscoelasticity, particularly for systems like hydrogels, rheometers provide critical data on storage (G') and loss (G'') moduli. To evaluate overall structural deformability, a key factor for tissue penetration, the extrusion method offers a straightforward, albeit low-resolution, assessment by forcing DDS through pores of a known size[24,25]. Furthermore, techniques like Fluorescence Recovery After Photobleaching (FRAP) are essential for characterizing the membrane fluidity of systems like liposomes and coacervates, which directly impacts receptor−ligand interactions[26−28].

A summary of these commonly used methods, along with their applicable systems, key parameters, and specific limitations within the context of DDS characterization, is provided in Table 1[28-36]. The rational selection and combination of these techniques are crucial for building a comprehensive mechanical profile of a DDS, which in turn informs the design principles for optimizing its *in vivo* performance.

3. Effects of mechanical properties on the *in vivo* fate and biological performance of DDS

The mechanical properties of DDS significantly influence their biological performance (Fig. 3), which can be broadly categorized into two major effects: 1) the mechanical adaptability of the delivery vehicle itself enhances biological adhesion and tissue penetration behavior, as well as boosts receptor−ligand interactions within organisms. For example, the interaction between the receptor and ligand is primarily enhanced by maximizing the interaction area and enabling their fluidity on both the delivery system and cell surface; 2) since organisms can recognize different mechanical stresses, the flexibility of the carrier affects its interactions with cells and activation of downstream signals, including cellular uptake and *in vivo* circulation. Taken together, these effects orchestrate the entire *in vivo* fate of a DDS, a multistage cascade from administration to therapeutic action. According to the physiological process of DDS *in vivo*, these biological performances are often evaluated based on six aspects: biological adhesion, blood circulation, tissue penetration, cellular uptake, receptor−ligand interactions, and mechanoimmunity and biocatalytic capabilities. Generally speaking, the stiffness of DDS affects their cellular uptake efficiency in the body, blood circulation time, and the ability of mechanical immune activation. Their structural deformability affects their tissue penetration behavior in the body. Their interfacial characteristics influence their self-healing ability and adhesion effect at irregular interfaces. This section discusses how the flexibility of the delivery system affects these internal physiological processes for the purpose of disease treatment.

3.1. Biological adhesion and self-healing behavior in local delivery

While many DDS are designed for systemic circulation, a distinct strategy involves engineering mechanical properties for localized action, such as adhering to and healing tissues. This represents a specific *in vivo* fate that bypasses the challenges of the bloodstream. Hydrogels, endowed with both bioadhesive and self-healing properties, have emerged as advanced DDS for wound repair and tissue regeneration. Their bioadhesion ability relies on synergistic mechanisms: 1) Chemical interactions, including

Table 1 Key characterization methods, applicable systems, advantages, and limitations for mechanically tuned DDS.

Method	Applicable systems	Key mechanical parameter(s)	Key advantages of DDS analysis	Limitations and challenges in DDS analysis
Atomic force microscopy (AFM)	Individual nanoparticles immobilized on a substrate (liposomes, EVs, micelles, etc.)[29,30]	Young's modulus,	• Nanoscale resolution: Enables imaging and mechanical characterization of single particles, providing the most direct individual information. • Physiological environment simulation: can be operated in a liquid environment to better mimic *in vivo* conditions.	• "Bottom effect": For ultra-soft materials, the rigid substrate can significantly influence measurements, leading to an overestimation of the modulus; model correction is required[28]. • Low throughput: Single-particle measurement is time-consuming, making it difficult to obtain statistical information from large samples.
Nanoindenter	Bulk materials and scaffolds[31,32], such as hydrogels, polymer scaffolds, tumor tissues	Young's modulus,	• High precision & sensitivity: compared to AFM, it provides more accurate measurements for harder materials with lower background noise. • Simplified sample preparation: has a higher tolerance for sample roughness.	• Not suitable for single nanoparticles: Primarily used for analyzing macro- or microscale bulk materials. • Model dependency: Analysis relies on mechanical models that assume material homogeneity, which may not be fully applicable to complex biological materials.
Rheometer	Viscoelastic bulk systems, such as hydrogels[33,34], emulsions	Shear modulus (G′ & G″), yield stress	• Bulk property assessment: Provides overall rheological information of the material, which is critical for evaluating the injectability and self-healing properties of hydrogels. • Dynamic mechanical analysis: can simulate mechanical responses under various physiological conditions.	• Large sample volume required: Cannot measure the mechanical properties of individual DDS particles; reflects only the average performance of the system. • Lacks microscopic information: Cannot reveal the mechanical differences in the microstructure within the system.
Extrusion method	Vesicular systems, such as liposomes, transfersomes.	Deformability	• Simple & high-throughput: a rapid, low-cost method for assessing the average deformability of a large population of vesicles. • High functional relevance: Directly mimics the process of DDS passing through narrow channels (*e.g.*, interstitial spaces).	• Low resolution: Does not provide precise modulus values and struggles to distinguish between particles with similar deformability[35,36]. • Destructive measurement: The process may cause vesicle rupture, affecting the accuracy of the results.
Fluorescence recovery after photobleaching (FRAP)	Systems with fluidic membranes or interiors, such as liposomes, micelles, cell membranes	Fluidity/lateral diffusion coefficient	• Dynamic process visualization: Directly measures membrane fluidity, which is crucial for understanding biological processes like ligand–receptor interactions and membrane fusion. • Non-invasive: can be performed on live cells or biomimetic systems in real-time.	• Qualitative or semi-quantitative: Typically used to compare relative fluidity rates rather than obtaining precise mechanical parameters. • Reliance on fluorescent labeling: The labeling process itself may interfere with the original properties of the system.

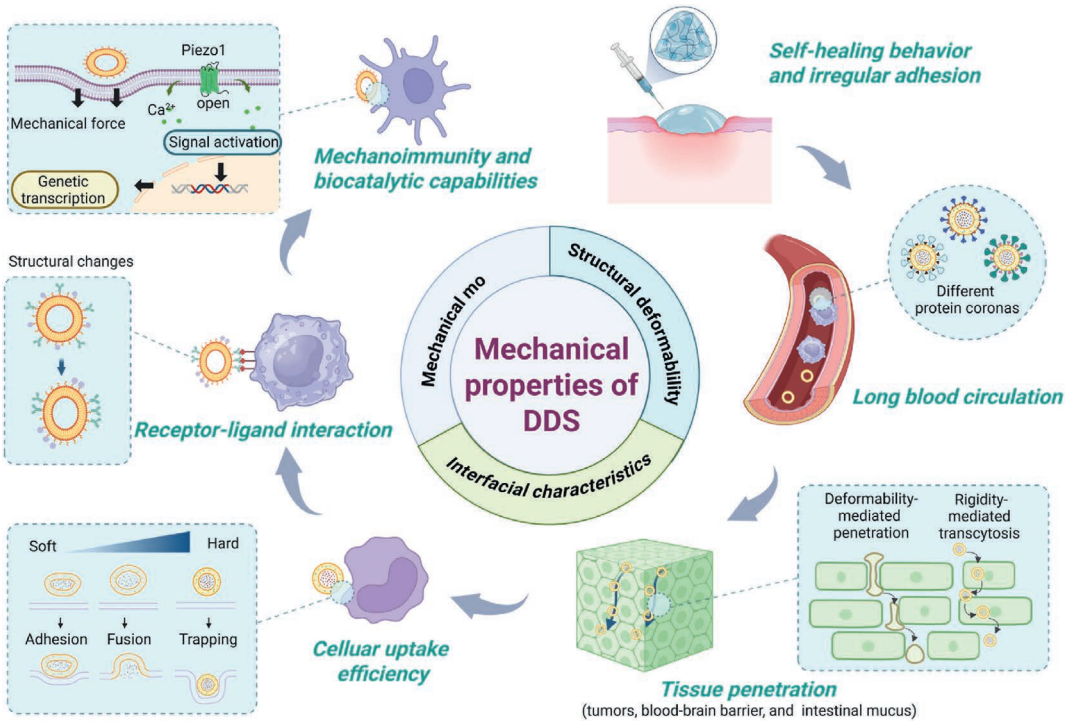

Figure 3 Illustration of the impact of mechanical properties on key physiological processes of DDS *in vivo*, including bioadhesion (*e.g.*, injectable gels), blood circulation, tissue penetration, cellular uptake, receptor−ligand interactions, mechanical signaling, and biocatalytic functions. Created in https://BioRender.com.

dynamic covalent bonds (*e.g.*, Schiff bases, disulfide linkages, NHS ester and amine coupling) that enable reversible binding to tissue surface groups (*e.g.*, $-NH_2$, $-SH$)[37-39], and metal-coordination bonds (*e.g.*, Fe^{3+}−catechol complexes mimicking mussel adhesion) for robust wet-tissue adhesion[40,41]. 2) Physical interactions, such as hydrogen bonding with collagen, hydrophobic anchoring in mucus layers, and electrostatic attraction between cationic polymers (*e.g.*, chitosan) and anionic cell membranes, contribute to adhesion[42-44]. 3) Mechanical interlocking, achieved *via* hydrogel swelling to conform to tissue microtopography, ensuring stable fixation[45]. 4) External energy-assisted adhesion (*e.g.*, ultrasound-induced cavitation), which enhances polymer−tissue entanglement for improved toughness and adhesion[46]. Notably, the self-healing mechanism of these hydrogels shares similarities with their bioadhesive properties, relying on reversible physical and chemical crosslinking (*e.g.*, dynamic covalent bonds, hydrogen bonding)[47,48]. The dynamic nature of these reversible networks enables hydrogels to maintain interfacial stability under physiological stress (adhesion strength typically 5−30 kPa), adapt to tissue motion, and apply gentle contractile forces to facilitate wound closure[38]. For example, catechol-modified chitosan hydrogels achieve 27.2 kPa adhesion strength with ~90% self-healing efficiency after cyclic loading[49].

In addition, some hydrogels exhibit self-growing behavior, where crosslink density or functional groups autonomously increase under external stimuli, enhancing mechanical and adhesive properties[50]. This mimics extracellular matrix (ECM) remodeling, facilitating host-implant integration and adaptive drug release. Key strategies include: 1) *in situ* polymerization of monomers (*e.g.*, acrylamide, NIPAM[51]); 2) bioinspired dynamic assembly (*e.g.*, mechanically trained PVA/tannic acid hydrogels achieving twofold expansion[52]); and 3) enzyme-triggered crosslinking (*e.g.*, glucose oxidase-mediated network densification for chronic wound management[53,54]). Remarkably, such hydrogels can adapt to cellular forces, promoting mechanotransduction on compliant substrates and even inducing osteogenic differentiation of mesenchymal stem cells, demonstrating the ingenious application of DDS to biomechanical forces[55].

Coacervates also possess biological adhesion and self-healing abilities, along with a strong loading capacity for biological macromolecules and various drugs. They can achieve targeted delivery and controlled release of various substances. The bioadhesive properties of coacervates have been experimentally validated in animal models, particularly demonstrating prolonged intestinal adhesion after oral administration for over 24 h[56]. The bioadhesion of coacervates can be regulated by changing the composition. Examples include the use of catechol-functionalized hydrophilic PEG shells. The stable adhesion of coacervates was ensured by reversible hydrogen bond interactions derived from catechol groups[57]. The dynamic nature of coacervates rendered them susceptible to environmental disruptions, with subsequent spontaneous reassembly occurring through inherent self-healing mechanisms. When the disruption ends, the components of coacervates can repeatedly aggregate through multivalent interactions and undergo rapid liquid−liquid phase separation (LLPS), restoring their previous state. This unique property has been leveraged for developing stimuli-responsive drug delivery platforms. When biomacromolecules, such as insulin were loaded into the coacervate, the release of insulin was linear under normal conditions. External ultrasonic stimulation induced instantaneous structural disintegration, triggering immediate burst release of payloads. Remarkably, the system underwent rapid structural reconfiguration within seconds upon ultrasound cessation, restoring baseline release kinetics. This switchable transition

between sustained and triggered release modalities presents promising potential for personalized therapeutic regimens requiring temporal dosage control[58].

3.2. Blood circulation and immune evasion in systemic delivery

For a systemically administered DDS, the *in vivo* fate begins in the bloodstream. This first hurdle is arguably the greatest: evading rapid clearance by the mononuclear phagocyte system (MPS). The mechanical properties of the DDS are key determinant of its ability to survive this surveillance and achieve prolonged circulation. Previous research has generally held that soft NPs can circulate in the bloodstream longer than stiff counterparts and accumulate more rapidly in the spleen, which can be used to increase tissue targeting and therapeutic efficacy[59]. This phenomenon is related to the reduced phagocytosis of soft DDS by macrophages, as their softness decrease the likelihood of being recognized and engulfed by the mononuclear phagocyte system (MPS)[14]. Additionally, the increased cell membrane tension needs to be maintained during phagocytosis, thus reducing the tendency to engulf these softer particles[60]. Miao et al.[15] developed NPs with a PEDGA hydrogel core coated with a red blood cell membrane. Due to their deformability, these NPs demonstrated a low affinity to plasma proteins and immunoglobulins, making them less likely to be engulfed by macrophages, thereby achieving prolonged circulation.

However, a recent study has identified a non-monotonic but clear dependence of the body circulation lifetime on the elasticity of NPs[61]. By dividing the stiffness of the NPs into three distinct regions: $<$15, 15−75, and $>$75 kPa, researchers found that, within the various regions, lower particle elasticity did correspond to longer blood circulation times. However, when comparing the NPs in different regions, the NPs with Young's modulus in the range of 15−75 kPa always showed the shortest circulation time. This finding contrasts with earlier studies that suggest softer particles always circulate longer. The difference may be due to the unconscious use of NPs with insufficient flexibility in previous experiments. This research offers a wide enough elastic range. Additionally, the study explored how the elasticity of NPs affects the formation of a protein corona, a layer of proteins that adsorb onto the surface of particles in the bloodstream. After incubating the NPs in mouse plasma for 12 h, the content and composition of adsorbed proteins were determined. It was found that the NPs with a modulus of 700−1700 kPa were less likely to adsorb proteins. Interestingly, the number and pattern of protein corona also varied based on NPs' elasticity. Further investigation demonstrated that ApoA1 was the key corona protein in the relationship between the body cycle life and the elasticity of NPs. ApoA1 tended to bind to NPs with Young's modulus in the 75−700 kPa range, rather than those that were too soft or too stiff. This study further explained the mechanism by which the elasticity of NPs regulates the body cycle life.

In summary, the elasticity of NPs directly influences their circulation time. Properly tuned DDS with optimal softness can evade phagocytosis, prevent protein aggregation, and maintain a prolonged presence in the bloodstream, thereby enhancing their therapeutic effects. In fact, the phenomenon that soft DDS are difficult to be engulfed up by MPS is closely related to their flexibility. The specific mechanism by which softness affects cellular uptake will be described in detail in the following text.

3.3. Overcoming biological barriers and tissue penetration behavior

After successfully navigating the systemic circulation, the next critical step for a DDS is to extravasate from blood vessels and penetrate deep into the target tissue, a process often hindered by physical barriers like the dense extracellular matrix (ECM). Various DDS with optimized deformability have been shown to enhance tissue penetration across various barriers, such as tumors, the blood−brain barrier (BBB), and the intestinal mucus due to their softness. The ability of DDS to adapt to their surroundings and their inherent elastically allow for deep and effective drug delivery. In the BxPC3-HPSC tumor model, liposomes with a Young's modulus of 19.9 MPa demonstrated the best penetration effect compared to both softer and stiffer formulations. This optimal level of flexibility allowed liposomes to deform into ellipsoidal shapes when attracted to different cellular environments. This elastic deformation helped them navigate through tight spaces and penetrate deep into tissues by moving from one corner to another under the influence of elastic deformation energy[62]. Regarding the reason why soft NPs have better dispersion, Yu et al.[63] attributed this phenomenon to their deformability, When attracted, these particles can transform into ellipsoids. This elastic deformation energy, in conjunction with the attraction from other corners, facilitated their movement from one corner to another. This research indicated that soft DDS showed good intestinal absorption, making them suitable for delivering drugs that are not typically amenable to oral application.

The flexibility of DDS not only helps them spread rapidly in the intestinal tract but also demonstrates excellent penetration effect in tumor tissue. The high interstitial fluid pressure (IFP) in tumors hinders the entry of most drugs from the vascular system into tumor tissues, which is a major challenge for the tumor delivery of nanomedicines[64]. The deformability of DDS promotes an increase in the curvature of NPs *in vivo*. Studies have shown that NPs with high curvature can effectively overcome elevated IFP that impedes particle exosmosis. Permeability experiments in Huh-7 xenograft tumors in BALB/c mice showed that NPs with the highest curvature were 12.2 times more permeable than spherical NPs. This enhanced permeability was attributed to the hopping-facilitated Brownian motion of NPs with high curvature in the physiological matrix. Moreover, the translational motion of NPs during diffusion was accompanied by obvious rotation, especially when the particles hopped from one cell in the network to another, indicating that the rotation of anisotropic NPs around the network chains fundamentally promoted their translational diffusion[11].

Moreover, while softness generally enhances tissue penetration, certain situations may benefit from moderately increased rigidity. Transcytosis is another mechanism through which drugs can pass the internal barrier, such as the BBB, tumor tissue, and the epithelial cell layer of the small intestine[65,66]. This process involves several processes, including mucus penetration, apical endocytosis, and basolateral exocytosis. After mucus penetration, NPs need to be endocytosed by the epithelium. Unlike mucus penetration, cellular uptake gradually improves as NPs rigidity increases. This trend also applies to the exocytosis phase of transcytosis. For example, research from Shen et al.[66] showed that increasing the stiffness of NPs can promote transcytosis between cells, thereby enhancing penetration across cellular layers. This suggests that a balance between deformability and rigidity is necessary to maximize the delivery of DDS, particularly when

targeting tissues like tumors or dense cellular barriers. Modifying ligands on the surface of NPs could promote the uptake and exocytosis of NPs by cells, and reduce the performance gap between hard and soft particles, which provides a potential strategy for improving the delivery efficacy of DDS[12,67].

Overall, the deformability of NPs highly affects their tissue penetration ability, enhancing their effectiveness. This is attributed to the fact that soft DDS can deform in complex biomechanical environments. While deformable and soft carriers are highly effective in penetrating barriers, tuning their stiffness based on the target tissue can further optimize drug distribution and therapeutic outcomes.

3.4. Cellular targeting, uptake, and intracellular trafficking

The final step in delivery is the interaction with and internalization by target cells. The mechanical properties of a DDS critically influence not only the efficiency of uptake but, more importantly, the pathway of internalization, which in turn dictates its intracellular fate and ultimate therapeutic action. The relationship between particle stiffness and cellular uptake efficiency is complex, with studies showing different results depending on the particle composition and the cell types involved[68]. While some research suggested that stiffer NPs were more easily taken up by cells, other studies reported that soft NPs were more readily internalized due to their deformability. This discrepancy highlighted the nuanced role that mechanical property plays in the uptake efficiency of DDS[69]. For example, the softer PEDGA nanogels with Young's modulus in the range of 10−3000 kPa were less likely to be taken up by tumor cells, endothelial cells, and macrophages[59]. Likewise, for PLGA-modified liposomes with Young's modulus in the range of 5−110 MPa, softer liposomes were not easily taken up by Caco-2 cells[70]. However, an opposite trend has also been observed in other studies. For the poly (*N*-isopropylmethacrylamide-disulfide bond-methacrylic acid) (P(NIPMAM-ss-MAA)) nanogels with stiffness ranging from 79 to 439 kPa, the softer the nanogel, the more likely it was to be taken up by tumor cells or cancer-associated fibroblasts[71]. Similarly, 85 MPa stiffness-transformable silica-based nanocapsules (SNCs) exhibited higher uptake by macrophages and tumor cells compared to 166 MPa SNCs[72]. The lack of consensus in these studies may stem from the use of various NP libraries with different material types, physicochemical properties, and different elastic ranges. There are also differences in the types of cells used in the experiments, leading to different mechanisms of NP endocytosis, which will affect the efficiency of endocytosis[73].

A recent study offers insight into how nanoparticle elasticity influences cellular uptake pathways[74]. This study found that soft NPs (<40 MPa) exhibited excellent deformability that resulted in only adhesion to the cell membrane and caused partial micropinocytosis. For NPs with moderate elasticity (40−100 MPa), cytoplasmic delivery was achieved through lipid rearrangement and membrane fusion with the help of their deformability and PEG polymer. For the hardest NPs (>100 MPa), due to their low deformability, they preferred to enter the cell *via* the classical lysosomal uptake pathway. Overall, the results suggested that the degree of elasticity affected the cellular internalization pathway: the softer Lipo-NPs adhered primarily to the cell membrane, the moderate Lipo-NPs tended to be membrane fused, and the rigid Lipo-NPs were preferentially endocytosed. This provided an explanation for the tendency of stiff NPs to be endocytosed. Studies have shown that NPs can inhibit clathrin-mediated endocytosis by suppressing the mRNA transcription of endocytogen-related proteins in RAW264.7 macrophages, including clathrin and adaptor protein complex 2 (AP-2)[75]. This is the mechanism by which stiffness affects clathrin-mediated endocytosis. In addition, the surface energy generated by deformation also plays an important role in the cellular uptake of soft DDS. Soft particles require greater surface energy, causing NPs to deform and adhere to the cell membrane[76]. Coacervates could enter cells *via* the lipid raft-mediated pathway to deliver mRNA and facilitate its successful expression. For instance, histidine-rich beak peptide (HBp)-based coacervates effectively delivered EGFP mRNA into HepG2 cells, with 72% of the cells exhibiting EGFP expression at 24 h post-transfection[77]. In conclusion, cellular uptake is not merely a physicochemical process. It involves interactions with membrane proteins, energy required for membrane encapsulation, endocytic protein synthesis, and intracellular transport. DDS with different mechanical properties (*e.g.*, flexibility) can affect the above various factors and reflect different cellular uptake trends.

Although in the previous text, it has been demonstrated that the cellular uptake behavior of NPs is stiffness-dependent, it is worth noting that ideal DDS must balance good endocytosis and dispersity in biological tissues. Experiments have shown that the ability of many DDS to disperse in biological tissues is often inversely related to their ability to be taken up by cells. For instance, although stiff NPs generally exhibit good endocytosis, their rigidity often comes at a cost. Stiff particles often struggle to disperse in biological environments, such as biohydrogels, which are essential for drug distribution within tissues[62]. Striking a balance between rigidity and softness is the key to optimizing cellular uptake in DDS. Therefore, although stiff NPs exhibit high endocytosis rates, their limited ability to disperse in tissues reduces their overall effectiveness. On the other hand, soft NPs may struggle with uptake but excel in tissue distribution. To overcome these challenges, modifications such as ligand attachment can be used to narrow the differences in uptake efficiency between soft and stiff particles. For example, by modifying liposomes with ligands, researchers can improve the uptake efficiency of softer NPs, making them more comparable to their stiffer counterparts[12]. Ultimately, NPs with moderate stiffness appear to offer the best balance, combining efficient endocytosis with improved tissue distribution. These findings suggest that the flexibility of DDS must be carefully tuned to achieve the desired therapeutic outcomes.

3.5. Receptor−ligand interaction

Delving deeper into the molecular level of cellular interaction, the fluidity and softness of a DDS can profoundly influence the binding dynamics between its ligands and cellular receptors, which precedes and facilitates uptake. The fluidity of the system can indeed disrupt the receptor−ligand multivalent interaction to elicit the mechanical signal, thus achieving anti-inflammatory or pro-inflammatory effects. This concept is supported by research that highlights the role of extracellular nucleic acid (NA) in forming complexes with endogenous NA antibodies, proteins, or cationic human antimicrobial peptides. Abnormal NA activates Toll-like receptors (TLR) to produce inflammatory cytokines, and NA complexes further promote the internalization of NA by immune cells to stimulate TLRs. This is a pathogenic mechanism in some autoimmune diseases[78-80]. A recent study has prepared arginine self-assembled coacervates with PEG shells, which could

trap NA, preventing it from binding to TLRs. When NA was contained within the coacervates, the fluidity of the system resulted in a close spacing between NA molecules (2.67 and 2.08 nm), which was much smaller than the size of TLR9 binding site (3.40 nm). This narrow space of the complex was unable to accommodate the TLR9 cavity to drive receptor clustering, which effectively inhibited the activation of inflammatory cells. The content of TNF, IL-6 and IL-1β decreased by 59%, 53%, and 44%, respectively, indicating that the coacervates effectively inhibited the activation of TLRs[81].

Furthermore, the softness of the system inhibits uptake and prolongs the action time of the receptor and ligand. For instance, research has demonstrated that the interaction between macrophage receptor MER-TK and phosphatidylserine (PS) was influenced by the softness of NPs[20]. Soft NPs (0.5 ± 0.1 kPa) can bind to macrophage cell membrane continuously, thereby inducing the effective expression of TNF-α protein in macrophage through mechanical stimulation and synergistic mechanism of PS receptor, indicating good anti-inflammatory activity. This "continuous binding" property also affected the cellular uptake kinetics and intracellular distribution of soft NPs. Previous studies have shown that endocytosis of elastic NPs was related to the binding strength between the membrane receptors and ligands on the surface of NPs[21]. Further studies showed that the hard NPs (100 kPa) were internalized into the cytoplasm after 3 h and almost disappeared after 12 h due to the degradation of macrophages. In contrast, soft NPs (2 kPa) remained 50% attached to the macrophage surface after 12 h. This demonstrated the ability of mechanical properties in DDS to regulate cellular uptake, which in turn regulates receptor−ligand interactions and downstream signaling pathways[22].

3.6. Eliciting biological responses through mechanoimmunity and biocatalytic capabilities

Beyond its role as a passive delivery vehicle, the final stage of the *in vivo* fate can involve the DDS functioning as an active therapeutic agent, directly modulating cellular behavior through its mechanical properties. Mechanoimmunity, which is defined as the coupling of biological mechanical signals and immune responses, is a recent research focus. It has been shown that mechanical signals can affect immune cells, including dendritic cells (DCs), T cells, and macrophages[82-85]. Mechanoimmunity mainly relies on signal transduction proteins that are sensitive to mechanical signals. Among them, the most representative one is PIEZO. PIEZO can sense mechanical signals and activate downstream signal transduction[86]. For instance, the attachment of the soft DDS on the surface of DCs generates mechanical stress, which activates the PIEZO1 mechanically sensitive ion channel and triggers Ca^{2+} influx. Then, the PI3K/Akt/mTOR pathway is activated to phosphorylate the interferon regulatory factor IRF3, promoting the production of type I interferons. In addition, the transcription of Edn-1 and the expression of inflammatory factors (IL-6, TNF-α, IFN-γ, etc.) are upregulated. Ultimately, this process induces continuous maturation of DCs and enhances T cell activation[87]. NPs with different stiffness have different effects on PIEZO. Soft NPs (81 MPa) induced slight membrane deformation, activated the PIEZO1 mechanical sensitive channel, and triggered Ca^{2+} influx. The latter activated calmodulin kinase CAMK2A, drived the phosphorylation of NF-κB, and promoted the release of pro-inflammatory factors, thereby transforming tumor-associated macrophages (TAMs) from M2 phenotype to M1 phenotype. However, hard particles (837 MPa) caused severe membrane deformation and high membrane tension, inhibiting the activity of PIEZO1 and preventing the activation of this pathway. Combining this characteristic with the high tissue penetration ability of soft particles, this combination could significantly inhibit tumor growth (with a volume reduction of more than 50%)[88]. Therefore, DDS can induce or suppress immune responses by adjusting biomechanical forces.

Moreover, various mechanically tuned DDS are capable of mimicking cellular morphology and functions. The deformability of DDS increases the contact area with organisms, while ensuring the mobility of receptors and ligands. Mechanical forces are integral to receptor−ligand signaling, especially in immune processes such as T cell receptor (TCR) activation. The fluidity of DDS could increase the multivalent interactions between receptors and ligands, enhancing mechanical signaling. In the case of TCR signaling, the mechanical interactions between TCR and its ligand, peptide-MHC, play a pivotal role in the activation of immune responses. Liposomes of conjugated immunosynaptic antibodies can act as artificial antigen-presenting cells (aAPCs). Due to the fluidity of lipid membranes, more ligands can be diffused to the regions where immune synapses are formed, enhancing multivalent interactions on the membranes. In a recent study evaluating the activation and expansion of mouse primary T cells, soft alginate aAPCs modified with anti-CD3 and anti-CD28, with a Young's modulus of 14.6 kPa (4.5 μm), were compared against highly rigid Dynabeads with a Young's modulus in the GPa range (4.5 μm). After three days of co-culture, the proliferation rate, cell volume, and the CD8/CD4 ratio of T cells in the presence of soft aAPCs increased by 1.5-, 1.45-, and 5.3-fold, respectively, compared to those treated with highly rigid Dynabeads[13].

In addition, soft DDS-based protocells can also form compartments to ensure an accelerated biochemical reaction. Drobot et al.[89] discovered for the first time that RNA catalysis was feasible in coacervates and further showed that coacervates could selectively retain longer RNA and concentrate oligonucleotides, which was conducive to biocatalysis. Subsequent studies showed that coacervates could enhance RNA catalysis by concentrating RNA molecules. At the same ribozyme concentration, the hammerhead cleavage reaction products in coacervates were 5−10 times higher than those in buffers[90]. Similarly, for hyperuricemia, using coacervates to load a ring catalytic system consisting of uricase and catalase could effectively degrade uric acid to allantoin and H_2O_2, while converting toxic intermediates to O_2 and H_2O. It could effectively reduce the damage caused by hyperuricemia[28].

3.7. Summary: mechanical properties orchestrate the in vivo fate of DDS

As delineated in this chapter, the mechanical properties of a DDS are not mere passive attributes but active determinants that govern its journey through the body, which constitutes its *in vivo* fate. The interplay between stiffness, deformability, and interfacial characteristics dictates a series of critical processes, often involving trade-offs that must be carefully balanced for optimal therapeutic outcomes.

1) Blood circulation: optimal softness, which is system-dependent and often in a non-monotonic relationship, minimizes protein corona formation and MPS uptake, thereby prolonging circulation half-life, a prerequisite for reaching the target tissue.

2) Tissue penetration: high deformability enables DDS to navigate through dense extracellular matrices, such as tumor stroma or mucosal barriers, by undergoing elastic deformation and leveraging hopping diffusion mechanisms. However, due to the inhibitory effect of softness on endocytosis, overly soft DDS are difficult to pass through biological barriers through transcytosis.
3) Cellular uptake: the efficiency and pathway of cellular internalization are profoundly stiffness-dependent. While excessive softness may lead to mere adhesion and frustrated phagocytosis, moderate stiffness often facilitates efficient endocytosis. The optimal stiffness is contingent upon the target cell type and the desired intracellular trafficking route.
4) Receptor−ligand interactions & signaling: interfacial fluidity and softness can potentiate or inhibit multivalent interactions, directly influencing downstream mechanotransduction pathways (*e.g.*, *via* PIEZO channels) and immune activation, thereby transitioning the DDS role from a passive carrier to an active signaling entity. In addition, the fluidity of DDS endows it with unique biocatalytic capabilities.

Consequently, the rational design of next-generation DDS necessitates a holistic view of this mechanical journey. A successful system might require a combination of properties, for instance, sufficient stiffness for efficient cellular uptake post-penetration, coupled with the deformability needed to reach the target cells in the first place. The case studies in the following chapter exemplify how this principled approach is being implemented across diverse platforms.

4. Engineering softness in major drug delivery platforms: case studies

To illustrate the power and universality of tuning mechanical softness as a design principle, this chapter will analyze its implementation across several DDS, including coacervates, hydrogels, Pickering emulsions, EVs, and liposomes (Table 2)[91-127]. Although these platforms differ fundamentally in their chemical composition and architecture, they converge on a common strategic approach: the deliberate engineering of mechanical properties to optimize biological performance. For each case, we will analyze the specific methods used to tune softness and illustrate how these mechanical adjustments directly dictate the system's *in vivo* fate and therapeutic efficacy.

4.1. Coacervates

Coacervates are a type of liquid droplets that form *via* phase separation of molecular driven by various weak interactions (Fig. 4A)[128]. They were first observed in 1929 in a solution containing oppositely charged biopolymers or isoelectric proteins with polyphenols[129]. Biomolecular coacervates play a key role in many cellular functions, including transcription, cell cycle control, and immune responses[130-132]. Their soft, liquid-like nature facilitates rapid molecular exchange, endowing them with unique advantages in drug self-loading and enhancing biochemical reaction rates[91]. As highlighted by Robert Langer and colleagues[133], coacervates represent an emerging delivery platform noted for its simplicity and efficiency. However, unmodified coacervates are prone to fusion, aggregation, and precipitation, hindering their biological application. To address this, they are often encapsulated within a membrane to form a core-shell structure. Unlike liposomes and EVs, coacervates exhibit time-dependent mechanical properties. The force required to achieve the same indentation depth varies over time. Similarly, their viscoelastic behavior also differs from that of covalently crosslinked hydrogels. Their G' and G'' spectra at low frequencies deviate from Maxwell's model, typically used to describe hydrogel viscoelasticity[134]. This behavior arises from the dynamic and reversible cross-linking between internal molecules. The network strength is lower than that of covalently crosslinked hydrogels. The cross-links within coacervates continuously associate and dissociate, creating a distinct stress relaxation pathway that enables network flow over extended timescales[135].

4.1.1. Diverse drug-loading capability

Coacervates can load a wide range of cargoes, including hydrophilic and hydrophobic drugs, as well as biomacromolecules. Previous studies have shown that coacervates in cells can concentrate the anti-tumor drug tamoxifen and affect its effectiveness[136]. Coacervates can be prepared by selecting appropriate components to facilitate the loading and protection of specific drugs[56]. For instance, emodin (EMO) presents challenges for oral delivery due to its low bioavailability, poor water solubility, and poor inherent targeting to disease sites. The coacervate microdroplets (Coac) can encapsulate EMO by a spontaneous enrichment process. EU S100, a commonly used enteric coating material, can be employed to protect the coacervates, forming EU-Coac. *In vitro* cell uptake experiments indicated that, compared with Coac and free coumarin 6, EU-Coac loaded with coumarin 6 showed significantly higher cellular uptake in RAW264.7 and NCM460 cells. Compared with the free drug or EMO@Coac, EMO@EU-Coac could modulate the macrophage phenotype by promoting CD206 expression, polarizing proinflammatory M1 cells into anti-inflammatory M2 cells (Fig. 4B)[56]. Animal experiments further revealed that EMO@EU-Coac possessed excellent anti-colitis efficacy. Compared with the other groups, EMO@EU-Coac significantly improved the colon length of mice. In terms of weight change, mice in the model group experienced a 32% loss after 10 days, while those in the EMO@EU-Coac group ceased to lose weight from Day 8, and even showed a slight weight gain. The results showed that coacervate DDS with EMO was more effective in treating colitis.

4.1.2. Efficient gene delivery

Coacervates are also effective for nucleic acid delivery, facilitating the cytoplasmic delivery of genetic materials. For example, a study delivered neurotrophin nerve growth factor (NGF) using a complex coacervate based on polyvalent trehalose[137]. The injection of NGF-loaded coacervate into the mouse striatum resulted in a significant increase in neuron size, suggesting their effectiveness in delivering bioactive proteins to nerve cells. Coacervate-based mRNA delivery systems offer several advantages, such as: 1) forming a physical barrier to protect mRNA from degradation by enzymes and nucleases; 2) enhancing mRNA pharmacokinetics, prolonging half-life and gene expression; 3) promoting the uptake of mRNA by cells through endocytosis; 4) promoting mRNA release into the cytoplasm for effective translation into proteins; 5) providing continuous and controlled doses of therapeutic mRNA, making it a viable option for gene therapy[137]. miRNA and DNA have also been successfully loaded into coacervates in some previous work to achieve *in vitro* and *in vivo* delivery[138].

Table 2 Representative DDS platforms and their composition, ways to adjust softness, mechanical parameters, applications and advantages.

Types	Composition	Ways to adjust softness	Mechanical parameters	Applications	Advantages	Ref.
Coacervates	PEG and TA	Multivalent interaction	/	Accelerate biochemical reactions	Superior ROS scavenging	91
	DEAE-dextran and PSS	Multivalent interaction	/	Anti-inflammatory	Enhanced cellular uptake	56
	Amphiphilic triblock polymer and mPEG-TK-PArg-b-PAsp	Multivalent interaction	/	Anti-inflammatory	TNF, IL-6, and IL-1β contents decrease by 59%, 53%, and 44%, respectively	81
	ε-Plys, PLGA, DPPC, DSPE-PEG and dsDNA	Multivalent interaction	/	Treatment of persistent hyperuricemia	Enhanced kidney accumulation	28
	PEG and hydrophobic core	Multivalent interaction	/	Treatment of diabetes	Controlled insulin release	58
	PEG and hydrophobic core	Multivalent interaction	/	Treatment of IBD	Long-term interface adhesion (>2 d)	57
	HBp	Multivalent interaction	/	Anti-tumor	Exhibit 74% EGFP expression at 24 h	77
Hydrogels	Alginate, CATNFC, QACs, PAM, Al^{3+}	CATNFC/Al^{3+} concentration	Compression modulus: 385 kPa	Wound healing	Adhesive, tough, antibacterial, cell affinity	92
	XG, SA-DA	Concentration/ratio adjustment	Adhesive strength: 24.5 kPa; elastic modulus: 1100 kPa	Wound healing; health monitoring	Injectable, conductive (0.65 S/m), antibacterial	93
	Chitosan, Ag^{+}, Cu^{2+}	CS/Ag^{+}/Cu^{2+} ratio	Adhesive strength: 4.3 kPa; elongation: 200%	Diabetic wound healing	Promotes cell migration, antibacterial	94
	O-HES, M-CMCS	O-HES/M-CMCS ratio	Adhesive strength: 25.7 kPa	Joint wound healing	Self-recoverable, promotes wound closure	95
	QCS, PDA/polyacrylamide	pH, QCS/PDA ratio	Tensile strength: 11.3−67.8 kPa; extensibility: 1154%	Chronic wound healing	Rigid-soft network, tissue adhesive, antibacterial	96
	Alginate, CATNFC, QACs, PAM, Al^{3+}	CATNFC/Al^{3+} concentration	Compression modulus: 385 kPa	Wound healing	Adhesive, tough, antibacterial, cell affinity	49
	γ-PGA-SH, HA-CHO	Polymer concentration	Compression modulus: 0.11 MPa; strain: 70%	Wound healing	Rheological stability, adhesive, antioxidant (85%)	97
	QCS, ODex	QCS/ODex ratio, DS of QCS	G′: ∼3000 Pa	Irregular and motion wounds healing	Good self-healing, antioxidant, antibacterial	98
	PL-Cat, ODex	PL-Cat/Fe/ODex ratio and pH	Storage modulus: 7600 Pa; compression stress: 80 kPa	Wound healing	Dissolvable, repeatable adhesion, removable	99
	Fe^{3+}, PEG, DOPA, PEGSD, HDI	Reactant concentration/ratio, temperature	G′: ∼ 2600 Pa	MRSA-infected wound healing, hemostasis	Adhesive, rapid self-healing, controlled degradability, antibacterial	100
	PEG-SG, TA, PNIPAM	Reactant concentration/ratio, temperature.	Tensile strength: 70 kPa	Wound healing, vessel-sealing	Ready-to-use, self-healing, time-enhanced adhesion	101
	PAA/BCD/PDA/polyacrylamide	Reactant concentration/ratio	Tensile strength: 21−51 kPa, strain: 899%−1047%	Antibacterial, wound healing	Ultra-stretchable, compressible, mild preparation	102
	Graphene/PC/PDA/CDL/Metformin	Reactant concentration/ratio	G′: 362 Pa	Hemostasis, diabetic wound healing	Self-healing, rheological stability	103
	Nanoclays/Phenylboronic acid/Chitosan/PDA	Reactant concentration/ratio, temperature	G': 462 Pa	MRSA-infected wound healing	Ultrafast self-healing, injectable, shape-adaptive	104
	Gelatin, PEG, PAM-PDA, Nanoclays	Reactant concentration/ratio, temperature, and pH	Good mechanical property	MRSA-infected wound healing	Injectable, tough, wet-adhesive, NIR-sensitive	105
	Cu@ZIF, GOx, Guar gum, MOF	Reactant concentration/ratio	Good mechanical property	Hemostatic, chronic or diabetic wound healing	Self-healing, antibacterial, hemostasis, antibiofilm efficacy	106
	MgFe-LDH, BMP, chitosan, silk fibroin	Reactant concentration/ratio	Enhanced storage & compressive moduli	Bone regeneration	Smart growth factor delivery for bone repair	107

	BAC/NIPMAM/MAA	Reactant concentration/ratio/ crosslinking density	Young's modulus: 82.92 kPa (soft)− 468.95 kPa (hard)	Anti-tumor	Deep tumor penetration	71
Pickering emulsions	PLGA, squalene	MW, particle conc., buffer, pH, oil conc.	Force-dependent deformation and dynamic fluidity	Vaccine adjuvant	Effectively stimulate humoral and cellular immunity	108
	Manganese NPs/aluminum hydroxide/AAV Vector/Squalene	Reactant concentration/ratio and stirring speed	/	Anti-infection/vaccines	Enhance viral vector vaccines at low doses	109
	Thiolated chitosan, parasin I, fish oil in water (92%)	Reactant concentration/ratio, temperature, and pH	/	Peritonitis	Improve gut microbiota(reduce harmful bacteria; increase beneficial bacteria)	110
	Chitosan/gum Arabia/rapeseed oil/MCT/Curcumin	Reactant conc./ratio, pH, stirring speed, ionic strength, temp.	/	Anti-inflammatory, antioxidant and antibacterial	High encapsulation efficiency and stability	111
	Chitosan/parasin I/water/fish oil	Reactant concentration/ratio, pH, and stirring speed	/	Peritonitis	Simple to prepare, antibacterial, and anti-inflammatory.	112
	Aluminum hydroxide, squalene	Buffer type and pH	/	SARS-CoV-2/Vaccine adjuvant	Potent humoral and cellular immune activation	113
	Aluminum hydroxide/PLGA/ PAA/Squalene	Reactant concentration/ratio/pH/ stirring speed	/	Anti-tumor	Superior anti-tumor efficacy; enhanced mRNA delivery	114
	PLGA/Ethyl iodized oil/anti-CTLA4	Reactant concentration/ratio	/	Anti-tumor	Boost tumor-targeted anti-CTLA4 delivery	115
	Albumin, squalene, lipopeptide ovalbumin	The minimum particle concentration	Young's modulus: 50 MPa	Anti-tumor	Potent lymph node delivery; robust anti-tumor cellular immune responses	116
Liposomes	DLPC, DMPC, DPPC, DSPC, DOPE, and DEPC	The phospholipid composition of the liposome	Young's modulus: 5.8−42.8 MPa	Anti-tumor	Good tumor penetration and cellular uptake	62
	C16:0-C18:1-PC, C18:0 C22:6-PC, C16:0-C18:1-PE, C18:0-C22:6-PE, C16:0-C18:1-PS, C18:0-C22:6-PS	The phospholipid composition of the liposome	Young's modulus: 116 and 188 kPa	Cellular uptake	Cellular uptake of 188 Pa liposomes is significantly increased	117
	PLGA, DSPE-PEG, soybean phospholipid, and cholesterol	Adding PLGA core	Young's modulus: 85−2118 kPa	Treatment of liver fibrosis	Better penetration and cellular uptake of medium hardness (712 kPa) liposomes.	12
	DOPC, DSPE-PEG, acrylamide and BA	Crosslinking agent content in hydrogel core	Young's modulus: 45 kPa−760 MPa	Systemic circulation	Prolonged circulation time (188 kPa)	61
	PLGA, DSPC, DSPE-PEG and cholesterol	Interfacial water volume	Young's modulus: 5 MPa, 50 and 110 MPa	Anti-tumor	Softer liposomes (5 MPa) are not easily taken up by Caco-2 cells	70
	DOPC, DSPE-PEG-mannose, Zn^{2+}, cGAMP and 5′-GMP	Cross-linked cGAMP and 5′-GMP encapsulated cores with $Zn(NO_3)_2$	Young's modulus: 15, 40, and 149 MPa	Anti-tumor	Potent immune response activation *in vitro* (40 MPa)	74
	DOPC and sodium alginate	Sodium alginate and calcium chloride	Young's modulus: 45 kPa−19 MPa	Anti-tumor	Enhanced cellular uptake in breast cancer cells	118
	PC and ethanol	Adding ethanol	/	Transdermal delivery of testosterone	Soft particles show stronger skin penetration ability	119
	DPPC and glycerol	Adding glycerol	/	Transdermal delivery of diclofenac sodium	High transdermal administration	120,121.
	DOPC and DPPS	PS content	Young's modulus: 0.5 and 80 kPa	Anti-inflammatory	Soft particles (0.5 kPa) continuously stimulate the macrophage receptor.	20

(*continued on next page*)

Table 2 (*continued*)

Types	Composition	Ways to adjust softness	Mechanical parameters	Applications	Advantages	Ref.
	PC, DPPS and cholesterol	PS content	Young's modulus: 2 and 100 kPa	Treatment of acute lung injury	Long-term adhesion on macrophages (12 h).	22
	DOPC, DPPC, cholesterol, DSPE-PEG and glycerol	W/O/W double emulsion droplets	FRAP experiments showed a higher diffusion rate	Immunotherapy	Potent immune activation (enhanced IFN-γ (28-fold), TNF-α (7-fold), IL-10 (17-fold), IL-2 (9.6-fold) in PBMCs)	122
	PC and KG	Surfactant	Extrusion method shows that the stiffness of liposomes is significantly reduced	Transdermal delivery of methotrexate	3−4 fold higher skin penetration than rigid liposomes	24
	PC, Tween 80, ethanol, sodium taurine cholate and oleic acid	The edge activator and ethanol	Extrusion method shows that TEL demonstrated the highest elasticity	Transdermal delivery of voricoanazole	High skin deposition (20.87%)	123,124
EVs	Cell-derived	Exosome-releasing cells grow in a soft gel	Young's modulus: 1 Pa	Anti-tumor	Better anti-tumor effect	125
	PLGA, DPPC and VE-based amphiphilic surfactant	NPs with cell incubation	/	Anti-tumor	High permeability and enhanced anti-tumor activity	126
	Cell-derived	EV derived from the human breast cancer cell line MDA-MB-231	/	Anti-tumor	To avoid low transcytosis in BBB	65
	Milk-derived and cholesterol	Adding cholesterol	Young's modulus: 1−8 MPa	Anti-tumor	The siRNA delivery efficiency was improved	127

Note: GelMA, gelatin methacrylate; NB, *N*-(2-aminoethyl)-4-(4-(hydroxymethyl)-2-methoxy-5-nitrosophenoxy) butanamide; HA-NB, hyaluronic acid-NB; LAP, lithium phenyl-2,4,6-trimethylbenzoylphosphinate; PEGDA, poly(ethylene glycol) diacrylate; Gox, glucose oxidase; Fe^{2+}, ferrous ions; G′, storage moduli; G′′, loss moduli; p(DMAEMA-DPAEMA), poly[2-(dimethylamino)ethylmethacrylate-*co*-2-(diisopropylamino)ethyl methacrylate]; PEGDA, polyethylene glycol diacrylate; LDH, layered double hydroxide; CS, chitosan/silk fibroin hydrogels; BAC, *N*,*N*′-bis(acryloyl)cystamine; NIPMAM, *N*-Isopropyl acrylamide; DLPC, 1,2-dilauroyl-*sn*-glycero-3-phosphocholine; DMPC, 1,2-dimyristoyl-*sn*-glycero-3-phosphocholine; DPPC, 1,2-dipalmitoyl-*sn*-glycero-3-phosphocholine; DSPC, 1,2-distearoyl-*sn*-glycero-3-phosphocholine; DOPE, 1,2-dioleoyl-*sn*-glycero-3-phosphoethanolamine; DEPC, 1,2-distearoyl-*sn*-glycero-3-phosphocholine; PC, phosphatidylcholine; PE, phosphatidylethanolamine; PS, phosphatidylserine; DSPE-PEG, 1,2-distearoyl-*sn*-glycero-3-phosphoethanolamine-*N*-[methoxy(polyethylene glycol)]; PLGA, poly(lactic-*co*-glycolic acid); DOPC, 1,2-dioleoyl-*sn*-glycero-3-phosphocholine; BA, *N*,*N*′-methylenebis (acrylamide); DSPC, 1,2-distearoyl-*sn*-glycero-3-phosphocholine; DPPS, 1,2-dipalmitoyl-*sn*-glycero-3-phospho-L-serine; KG,dipotassium glycyrrhizinate; ε-Plys, ε-polylysine; DEAE-Dextran, diethylaminoethyl glucan hydrochloride; DS, degree of substitution; CEA, 2-carboxyethyl acrylate; HMPP, 2-hydroxy-2-methylpropiophenone polyphenylate; HBp, histidine-rich beak peptide; GMA, lycidyl methacrylate; DAGM, ethylenediamine modified glycidyl methacrylate, CATNFC, cationized nanofibrillated cellulose; PAM, acrylamide and acrylic acid; XG, xanthan gum; OSA-DA, dopamine-modified oxidized sodium alginate; BG, bioglass; O-HES, oxidized hydroxyethyl starch; M-CMCS, modified carboxymethyl chitosan; QCS, quaternized chitosan; PDA, polydopamine; γ-PGA-SH, thiol-modified poly (γ-glutamic acid); HA-CHO, oxidized hyaluronic acid; QCS, glycidyl trimethyl ammonium chloride-graft- chitosan; PL-Cat, catechol-modified ε-poly-L-lysine; ODex, oxidized dextran; PEGSD, poly(glycerol sebacate)-*co*-poly(ethylene glycol)-*g*-catechol prepolymer; HDI, UPy-hexamethylene diisocyanate; PEG-SG, *N*-hydroxysuccinimide glutarate; TA, tannic acid; pDADMAC, poly(diallyl dimethyl ammonium chlorid; BC-*g*-pDADMAC, brushes grafted bacterial cellulose nanofibers; PEGS-PBA-BA/CS-DA-LAG, denoted as PC, phenylboronic acid and benzaldehyde bifunctional polyethylene glycol-*co*-poly(glycerol sebacic acid)/dihydrocaffeic acid and L-arginine cografted chitosan; MOF, metal-organic frameworks; HAG, hexanoylated agars; HAS, human serum albumin; EDC·HCl, 1-ethyl-3-(3-dimethylaminopropyl) carbodiimide hydrochloride; MW, molecular weight; MCT, medium chain triglyceride.

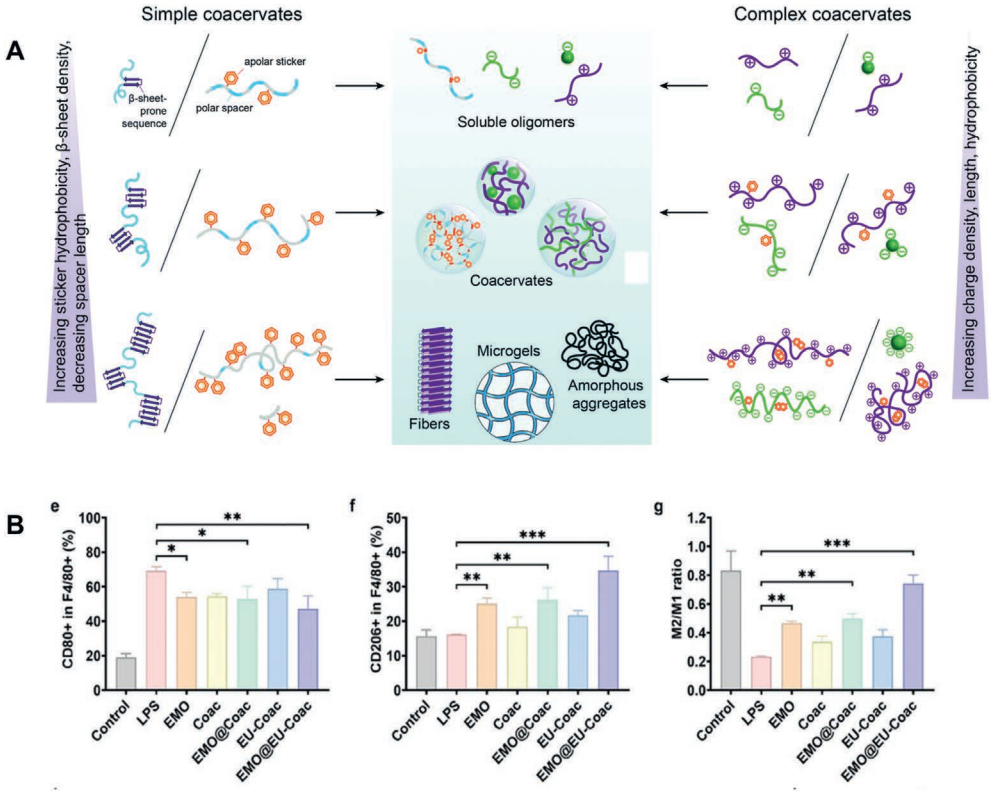

Figure 4 Coacervates serve as versatile and soft platforms for drug delivery. (A) The composition of the coacervates. Reprinted with the permission from Ref. 128. Copyright © 2021 Royal Society of Chemistry. (B) Phenotypic analysis of macrophages treated with different groups. Reprinted with the permission from Ref. 56. Copyright © 2024 Wiley.

In a recent study, coacervates can efficiently deliver mRNA directly into the cytoplasm[77]. Researchers efficiently delivered mRNA into cells using histidine-rich beak peptide (HBp) coacervates conjugated with a disulfide self-destructive group, which decomposed in the reducing intracellular environment to release payloads. Transfection studies with EGFP mRNA in HepG2 and HEK293 cells showed exceptional uptake (∼98% and 94.8%, respectively) and high EGFP expression (72% and 81.6% after 24 h), indicating their potential as gene therapy vectors. Critically, these coacervates protected encapsulated mRNA from degradation (resisting 1 mg/mL RNase for 2 h) and utilized a unique, non-endocytic uptake pathway—evidenced by insensitivity to the energy pathway inhibitor NaN_3, allowing direct cytosolic delivery and bypassing endosomal escape, unlike conventional NPs such as liposomes, EVs, or hydrogels.

In a subsequent mechanistic study, the authors identified the exact mechanism by which coacervates are taken up by cells. The coacervates were captured by filopodia-like protrusions, which decorate the cell surface in a manner similar to phagocytosis[139]. The droplets then sank into the cell through progressive deformation and topological rupture of the plasma membrane. This is an active process driven by energy-dissipating cytoskeleton remodeling. In addition, the presence of cholesterol can increase bending rigidity and binding to the membrane, promoting coacervate-membrane interaction, which in turn increases uptake efficiency. This research highlighted the significance of flexibility as a critical parameter of coacervates.

In previous studies, the relationship between the efficient nucleic acid delivery of coacervates and their flexibility has not been clearly explained. A recent study showed that when nucleic acids were loaded into coacervates, the coacervates became softer[140]. This is because the binding of nucleic acids with internal molecules induces local expansion, transforming the coacervates into a dynamic state and significantly enhancing molecular migration. AFM measurements confirmed that coacervates became softer after nucleic acid loading, and the loading process was accompanied by a significant transition of the internal structure from rigidity to flexibility.

4.1.3. Accelerated biochemical reactions as protocells

In addition to drug delivery, coacervates can function as artificial protocells or membraneless organelles, regulating the occurrence of various biochemical reactions[128]. Dipeptide-based coacervates can serve as biological microreactors, enabling diverse catalytic reactions, including photocatalysis and transition metal catalysis, in aqueous environments. These coacervates exhibited effective loading capacity for a wide range of macromolecules and other components, including hydrophobic catalysts. By encapsulating the catalytic substances, coacervates enabled a chemical reaction that was not normally feasible in aqueous solutions[141]. Furthermore, coacervates have been used to deliver specific enzymes to trigger biological reactions. The specific method of constructing the protocell was detailed in a previous study[142]. For instance, the researchers formulated polylysine−polynucleotide complex coacervate droplets to treat hyperuricemia.

To enhance biocompatibility, the coacervate droplets were coated with a PEGylated phospholipid membrane and loaded with a catalytic system (Uri and catalase) that efficiently degraded uric

acid into allantoin and H_2O_2 while converting toxic intermediates into O_2 and H_2O, with the generated O_2 further promoting uric acid degradation. Fluorescence imaging revealed significantly higher renal accumulation of the catalytic coacervates compared to the free enzyme system, attributed to their flexibility and deformability. In hyperuricemic mice, this drug delivery system effectively alleviated hyperuricemia and prevented the significant increase in renal injury biomarkers (KIM-1 and NGAL) observed in model mice, demonstrating its efficacy in reducing hyperuricemia-induced kidney damage[28].

4.1.4. *Regulate cell behavior through biomechanical forces*

The intrinsic stiffness of coacervates can also be harnessed to regulate mechanical stimulation to cells, thereby regulating cell behavior. In a recent study, a biomimetic ECM was established through heterogeneous hydrogels derived from coacervates. The rigid network of the biomimetic ECM provides anchor points to support the mechanical sensing of cells. It effectively promoted the diffusion of stem cells and enhanced mechanical sensing. The experimental results showed that the expression of mechanical sensing markers (PTK2, vinculin, integrin β1) of stem cells grown in biomimetic ECM was significantly upregulated, and enhanced nuclear translocation of mechanosensitive transcription factors was observed. In future research, drugs can be loaded into coacervates to jointly regulate cell behavior through both mechanical stimulation and drug effect[143].

In conclusion, coacervates can represent a soft platform for drug delivery, gene therapy, and artificial organelle construction, opening avenues for innovative therapeutic strategies in various biomedical applications. As a relatively new delivery system, the mechanisms through which coacervate flexibility influences cellular uptake are still being elucidated. The mechanism for regulating the flexibility of coacervates also requires in-depth research. As mentioned above, their softness, which promotes of their interaction with the cell membrane is a notable example.

4.2. *Gels*

Gels are soft materials with a three-dimensional cross-linked polymer network, characterized by high water content, tunable mechanical flexibility, and biocompatibility[144-146]. This inherent flexibility enables gels to conform closely to tissues, reducing irritation and facilitating controlled, sustained drug release, thereby enhancing therapeutic efficacy and minimizing side effects in localized treatments. By fine-tuning factors such as the degree of crosslinking, polymer composition, and the incorporation of responsive elements, researchers can modulate the mechanical properties of nanogels to optimize their performance[147]. For example, reducing crosslinking density results in softer nanogels, thereby better adapting to tissue microenvironments. Increasing crosslinking enhances rigidity for applications that require high structural stability. This tunable flexibility is crucial in customizing drug release profiles for specific therapeutic needs. Based on specific application requirements, soft gels can be categorized into self-healing gels, injectable gels, responsive nanogels, soft matter gels and others[148-150]. Each category displays unique characteristics related to their adaptive behavior, mechanical properties, and response to external stimuli.

4.2.1. *Good biocompatibility and dynamic adhesive behavior*

Self-healing and injectable gels offer unique advantages in biomedical applications. Self-healing gels provide significant advantages in chronic wound care. Wang et al.[151,152] developed a photothermal-responsive, self-healing hydrogel dressing composed of structural color microspheres (CMPs) that adhered and adjusted stiffness under near-infrared (NIR) irradiation. This thermoreversible property, softening at 42 °C, enhanced flexibility and allowed controlled release of co-loaded Eumenitin and VEGF, thereby promoting angiogenesis and antibacterial effects and expediting wound healing. Unlike traditional rigid materials, the soft structure of CMPs enabled real-time drug release monitoring *via* visible color changes, creating a responsive system for precise wound treatment. Other examples include self-growing hydrogel bioadhesive (sGHB)[53], which strengthened over time to control inflammation and support tissue regeneration, and SMART-EXO bioactive microgel[153], which promoted healing through dynamic adhesion and self-contraction.

Building upon the advantages of self-healing hydrogels, injectable hydrogels offer additional benefits by allowing for minimally invasive delivery and *in situ* formation within biological environments. They facilitate this approach through *in situ* gelation, ensuring precise drug release with biocompatibility and mechanical adaptability[154]. These properties make them highly suitable for applications such as tissue engineering, biosensing, and localized therapy. For instance, Tang et al.[155] introduced a "metagel" sensor for real-time intracranial monitoring using stimulus-responsive hydrogels. The metagel adapted its softness to physiological stimuli, shifting ultrasound reflection frequencies for wireless measurement. With a 10 cm detection depth and full degradation within 18 weeks, this system enabled accurate, non-invasive measurements. Similarly, Wang et al.[156] developed adaptive microdrugs capable of crossing the BBB through receptor−ligand binding and deformation-mediated endocytosis, optimizing glioblastoma targeting. Other innovations include Liu et al.'s[157] pH-responsive hydrogels for deep-tissue ultrasound monitoring and Weng et al.'s[107] thermal-responsive hydrogels for enhanced bone regeneration. These innovations exemplify the broad potential of injectable gels in precise, soft, and minimally invasive therapies[158].

4.2.2. *Optimized blood circulation through "hard blocking and soft delivery" strategy*

Nanogels, with tunable softness and nanoscale size (<200 nm), efficiently cross biological barriers and enhance drug delivery[159,160]. Compared to rigid NPs, soft nanogels can prolong circulation time, improve targeting, and enhance drug efficacy[161,162]. The flexibility of nanogels plays a crucial role in drug delivery. Soft nanogels can evade rapid immune clearance more effectively than rigid ones, which prolongs systemic circulation and enhances target-site accumulation. Their responsiveness to internal stimuli (*e.g.*, pH shifts, redox gradients) and external triggers (*e.g.*, ultrasound, temperature) enables controlled, site-specific drug release, minimizing off-target effects and optimizing therapeutic outcomes. For instance, Sun et al.[163] developed ultrasound-responsive nanogels for triple-negative breast cancer therapy. Initially rigid, these nanogels accumulated at tumor sites but softened upon ultrasound exposure, facilitating deeper tumor infiltration, enhanced drug release, and reduced systemic toxicity. Similarly, Bhatia et al.[164] designed soft multivalent nanogels for influenza therapy, achieving a 400-fold efficacy increase over their rigid counterparts.

A notable strategy leveraging nanogel stiffness in drug delivery is the "hard blocking and soft delivery" approach (Fig. 5A)[75]. By adjusting the ratio of *N*,*N*′-bis(acryloyl)cystamine and *N*-

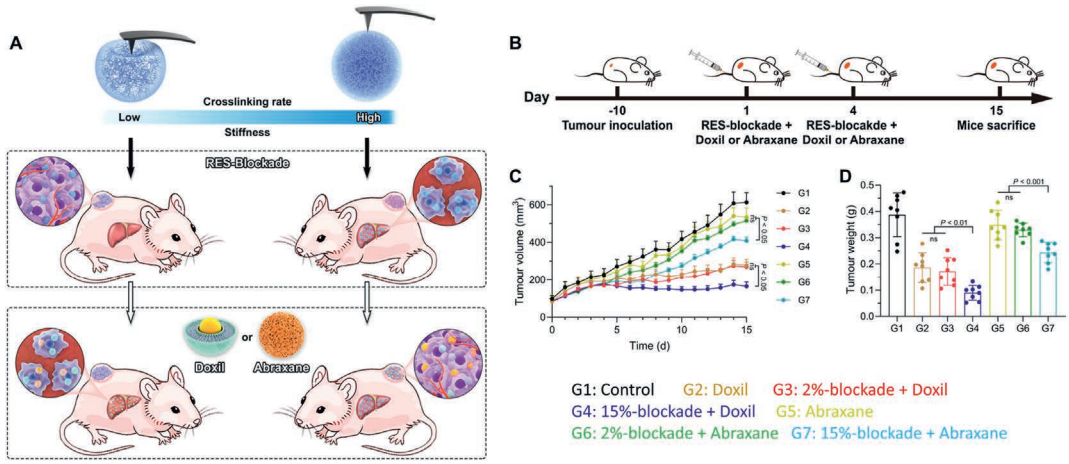

Figure 5 A sequential administration strategy based on nanogel stiffness achieves enhanced tumor accumulation and suppression. (A) Illustration of the "hard blocking and soft delivery" drug administration strategy. (B) The drug administration strategy in mice. (C, D) The tumor volume and tumor weight changes in mice treated with different formulations. Reprinted with the permission from Ref. 75. Copyright © 2023 Springer Nature.

isopropylmethacrylamide, researchers engineered stiffness-tunable nanogels, generating rigid (15% NG) and soft (2% NG) variants. This method first employed rigid nanogels to transiently block the reticuloendothelial system, reducing macrophage uptake and prolonging hepatic retention. Subsequently, softer nanogels were introduced, enabling deeper tumor penetration and enhanced accumulation, ultimately improving tumor suppression (Fig. 5B−D). Notably, softer nanogels encapsulating indocyanine green (ICG@2% NG) in combination with mild photothermal therapy effectively disrupted tumor-associated fibroblasts and degraded the extracellular matrix, remodeling the tumor microenvironment and further enhancing the therapeutic efficacy of stiffer nanomedicines[71]. These findings suggest that the integration of nanogel mechanics into cancer therapy may offer potential benefits, including modulation of macrophage activity, optimization of tumor microenvironment interactions, and enhanced drug delivery efficiency. Further research is needed to fully explore these possibilities in the development of next-generation nanomedicine.

4.2.3. Mechanical signal transmission in precise monitoring and T cell activation

Soft matter gels, with a low mechanical modulus and high flexibility, are well-suited for applications in soft electronics, wearable devices, and biosensors, as they can conform to dynamic body movements and environmental changes[165-167]. This mechanical compliance supports real-time physiological monitoring, which is vital for continuous health assessments like glucose tracking and early disease detection[165,168,169]. In soft electronics, these gels enhanced soft circuitry and sensor integration. Liu et al.[170], for instance, designed a compliant hydrogel biointerface that anchors wireless pressure sensors to dynamic tissues, addressing mechanical mismatches for continuous intracranial pressure monitoring. Similarly, Zhao et al.[171] introduced a self-healing GaInSn/Ni composite hydrogel with magnetic field-soft flexibility, enhancing strain sensing for body motion monitoring and nearly doubling EMI shielding from 31.8 to 62.5 dB. Furthermore, Bao et al.[172] developed a wireless smart bandage featuring dual-conducting hydrogel with thermally controlled adhesion, which provided a secure yet removable fit for wound surfaces, facilitating continuous monitoring and improving wound healing by 25% and dermal remodeling by 50%. These innovations highlighted the potential of soft matter gels in healthcare for soft, precise monitoring, and responsive therapy.

Beyond biosensing, the mechanical properties of soft gels play a critical role in generating biomechanical signals and regulating T cell activation, making them valuable tools in immunotherapy[173]. T cell activation relies on TCR stimulation *via* pMHCs or anti-CD3 antibodies, alongside CD28 costimulation. Wang et al.[13] developed alginate-based aAPCs with tunable stiffness, demonstrating that softer aAPCs (Young's modulus: 14.6 kPa) enhanced mouse T cell proliferation by 1.5-fold and increased the CD8/CD4 ratio by 5.3-fold compared to rigid Dynabeads (Young's modulus in the GPa range). Similarly, artificial lymph node matrices with stiffness ranging from 0.5 to 10 kPa optimized T cell expansion, with softer microparticles (2 kPa) significantly improving T cell proliferation[174]. Soft hydrogels also supported T cell viability and cytokine release by mimicking native tissue environments. They enabled T cell-mediated gel degradation for controlled microparticle release and *in situ* expansion, ultimately enhancing antitumor efficacy[175-177]. Recent studies further demonstrated that gel-mediated mechanical forces directed stem cell differentiation (*e.g.*, hepatic lineage) *via* YAP signaling[178]. Collectively, these findings underscore the potential of gel softness and adaptability in advancing immunotherapy and drug delivery.

4.3. Pickering emulsions

Emulsions are dynamic and soft delivery systems widely applied in pharmaceuticals, cosmetics, and the food industry[161,179]. They consist of two immiscible liquids, typically oil and water, stabilized by emulsifiers that reduce interfacial tension. Among the various types of emulsions, Pickering emulsions represent an innovative strategy for enhancing immune cell activation and improving drug delivery efficiency. The flexibility of Pickering emulsions stems from both mechanical properties, such as rheology, viscoelasticity, and interfacial plasticity, and compositional factors, including droplet size and interfacial tension[180]. These properties enable adaptation to complex biological environments, improved tissue penetration, and efficient drug

encapsulation, controlled release, and targeted delivery. Key emulsion types, such as oil-in-water (O/W), water-in-oil (W/O), and multiple emulsions, can be tailored based on solubility and release requirements to optimize therapeutic outcomes[181].

Unlike traditional emulsions stabilized by surfactants, Pickering emulsions are stabilized by solid particles that adsorb at the oil-water interface to form stable structures[182-185]. Their mechanical properties, including softness and fluidity, can be fine-tuned by adjusting the size, concentration, or type of stabilizing particles, enhancing their compatibility with biological systems and expanding their applications in drug delivery[186-189]. For instance, softer emulsions can be achieved by using smaller, more deformable particles or by adjusting the concentration to allow greater fluidity in the continuous phase. The synergistic interplay between fluidity and permeability enhances the performance of Pickering emulsions as a soft drug delivery platform. Fluidity enables dynamic deformation and improved mobility, optimizing processes such as antigen uptake, cellular interaction, and immune activation. Simultaneously, permeability, driven by tunable interfacial properties and droplet deformability, facilitates deep tissue penetration and precise targeting of challenging sites such as tumors and lymph nodes. This review emphasizes Pickering emulsions due to their potential for targeted drug delivery and bioavailability enhancement, making them a promising platform for innovative therapeutic strategies.

4.3.1. Pathogen-mimicking structure and immune cell activation

The fluidity of Pickering emulsions plays a pivotal role in optimizing antigen delivery and immune activation by promoting dynamic interactions between antigen-loaded droplets and cell membranes[113,190]. This enhanced antigen uptake by APCs, supporting gradual release, and stimulated both humoral and cellular immune responses. Ma's group[190] developed a force-responsive Pickering emulsion adjuvant system stabilized by PLGA particles (PPAS), which exhibited lateral mobility and deformation upon interaction with APCs (Fig. 6A−D). This mechanosensitive behavior enhanced antigen presentation and immune activation, with optimal antigen-loading efficiency observed at specific particle concentrations. Similarly, alum-stabilized Pickering emulsions have been used as malaria vaccine adjuvants, mimicking pathogen dynamics to improve antigen uptake and presentation by immune cells[191]. Chitosan nanoparticle-stabilized Pickering emulsions (CSPE) further demonstrated enhanced endocytosis and antigen cross-presentation, leveraging a pH-sensitive transition mechanism to optimize antigen release and enhance immune responses[192].

To address the COVID-19 pandemic, Ma's team[113] designed particulate alum microgel-stabilized Pickering emulsions (PAPE), which outperformed traditional alum-based adjuvants in DC activation and immune response. The deformability and fluidity of PAPE contributed to a balanced Th1/Th2 immune response, elevated antibody titers, and enhanced T-cell activation. Additional studies revealed that surface-located particles (CNP-S) promoted slower migration, favoring antigen retention and T-cell activation, while faster-migrating inside-droplet particles (CNP-I) bolstered humoral immunity[193]. Other studies underscored the versatility of these emulsions. Sha et al.[194] demonstrated that soft particle-stabilized emulsions promoted lysosomal escape, boosting T-cell responses. Du et al.[195] utilized these emulsions to deliver MPLA, enhancing antitumor immunity. Wu et al.[114] developed CaP-stabilized Pickering emulsions for mRNA vaccine delivery, achieving enhanced $CD8^+$ T-cell activation. Additionally, Cao et al.[196] employed alum-stabilized emulsions for sequential antigen delivery, strengthening both innate and adaptive immunity in cancer models.

Collectively, these findings highlight the transformative potential of Pickering emulsions in immunotherapy and vaccine development. By mimicking pathogen dynamics, enhancing antigen mobility, and fine-tuning immune activation, they offer a highly soft platform for next-generation vaccines and therapeutics. Their tunable properties and ability to boost immune responses position Pickering emulsions at the forefront of innovative drug and vaccine delivery systems.

4.3.2. Deep tissue penetration for improved efficacy

Pickering emulsions exhibit exceptional potential in enhancing tissue and cellular penetration, a critical factor for targeting challenging tissues such as tumors and lymph nodes. Their tunable interfacial properties enable deep tissue penetration and effective drug delivery. For instance, Yang et al.[197] developed a gold nanocluster (Au NC)-stabilized emulsion with tunable interfacial properties. The hydrophobic dye-modified Au NCs formed amphiphilic particles, reducing interfacial energy and stabilizing the emulsion. This system created dynamic interfacial microdomains capable of adapting to cellular membrane structures, enabling direct penetration without membrane disruption. Such adaptability not only promoted cellular uptake but also enhanced photothermal therapeutic outcomes, establishing Pickering emulsions as a potent tool in cancer treatment.

Similarly, Chen et al.[198] engineered fruit-derived EVs-stabilized structural droplet drugs (ESDDs) for glioblastoma treatment. The dense vesicle coverage at the droplet interface improved deformability and enhanced membrane contact, facilitating superior cellular uptake and deeper tumor penetration. By modulating vesicle concentration, researchers achieved a balance between droplet flexibility and therapeutic performance, demonstrating the adaptability of ESDDs in addressing complex therapeutic challenges.

In vaccine delivery, deformable albumin-stabilized emulsions (DASEs) exemplified the significance of emulsion deformability[116]. These emulsions, optimized to approximately 330 nm, efficiently navigated interstitial spaces and lymphatic barriers, enabling precise lymph node targeting. This design fostered antigen depot formation, enhanced cross-presentation, and stimulated robust cytotoxic T lymphocyte responses. Notably, DASEs facilitated a 314% increase in IFN-γ secretion and extended survival in tumor models, underscoring the pivotal role of deformability in vaccine efficacy. Wang et al.[192] developed a water-in-oil Lipiodol Pickering emulsion (LPE) stabilized by calcium carbonate NPs and hemin, encapsulating lipoxygenase (LOX) (Fig. 6E)[199]. The emulsion's flexibility was adjusted *via* pH modulation; lower pH enlarged droplet size and accelerated LOX release. This pH-responsive behavior enhanced drug retention at embolization sites, significantly improving therapeutic outcomes compared to conventional Lipiodol emulsions, reflecting the intelligence of soft DDS.

4.4. Extracellular vesicles

In 1967, Peter Wolf pioneered the discovery of EVs, identifying 20−50 nm vesicles derived from platelets that secrete clotting inhibitors[200]. This finding laid the groundwork for the understanding of EVs, which were subsequently divided into distinct subtypes in subsequent studies, including microvesicles,

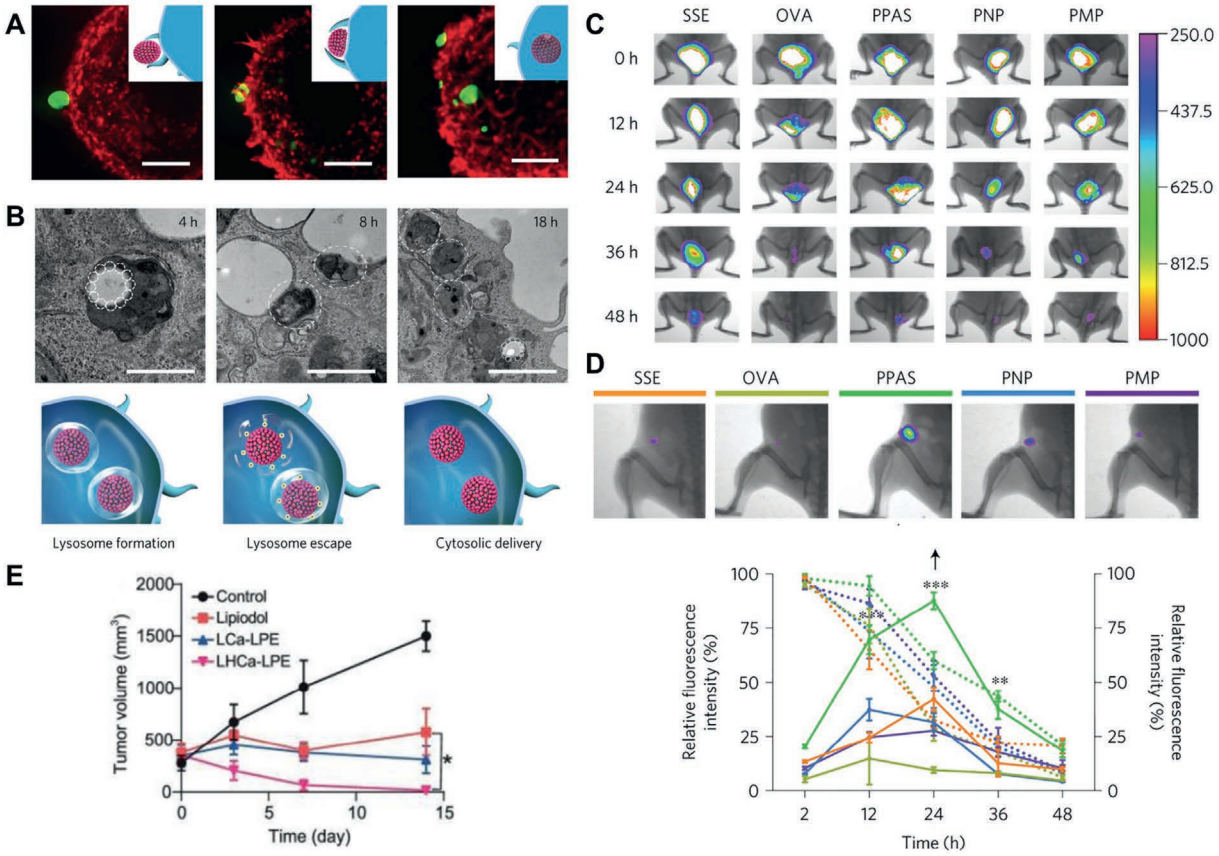

Figure 6 The deformability and dynamic fluidity of Pickering emulsions enhance antigen delivery for potent immune activation and therapeutic efficacy. (A) The process of BMDCs phagocytizing the PPAS/OVA complex. Membrane actin and OVA were labeled with Rhodamine-penicillin (red) and Alexa Fluor 488 (green), respectively. Scale, 5 μm. (B) The intracellular distribution of PPAS was observed by TEM and schematic diagrams at the specified time. Scale, 5 μm. (C) The continuous fluorescence intensity of the antigen varies over time. OVA was labeled with Cy7. (D) The presence of the antigen in the draining lymph nodes at 24 h, as well as the quantitative fluorescence intensity of the antigen at the injection site (dotted line) and dLNs (solid line). Reprinted with the permission from Ref. 190. Copyright © 2018 Springer Nature. (E) The average tumor growth curves of tumor-bearing rats with N1S1 tumors in different treatment groups. Reprinted with the permission from Ref. 199. Copyright © 2023 Oxford University Press.

exosomes, and apoptotic bodies according to their morphological characteristics and contents[201]. The biological mechanisms of EV generation are different, as they can either bud directly from the plasma membranes or be released through exocytosis after the formation of vesicles inside the cells[202]. Due to homologous targeting and flexibility, EVs have been regarded as promising vehicles for drug delivery.

EVs have many advantageous features. For example, they are capable of encapsulating and protecting nucleic acids, and delivering them to the recipient cells. Furthermore, their negatively charged surfaces, coupled with the presentation of the surface protein CD47, enable them to avoid the mononuclear phagocyte system (MPS), thus exhibiting intrinsic stability in the circulation. In addition, they may exhibit inherent targeting properties determined by their lipid composition and protein content, which may compensate for the shortcomings of synthetic delivery systems (Fig. 7A)[203,204].

4.4.1. Adjusting the softness of EVs by modulating parent cells

The flexibility of EVs is intricately related to the state of the parent cells from which they are derived. Research employing AFM has shown that the mechanical properties of EVs derived from malignant cells exhibited reduced stiffness, possibly due to their greater abundance of membrane proteins, which softened the membrane by making it thinner[205]. This trend was echoed in studies of gastric cancer cells, where the Young's modulus of EVs derived from normal and malignant cell lines varied significantly, demonstrating the influence of tumor characteristics on EV properties. Specifically, the Young's modulus of EVs derived from GES-1, HMrSV5 (normal cell lines), AGS, HGC-27, and MGC-803 (gastric cancer cells with different malignancies) cells were 13.5, 8.6, 6.5, 4.6, and 4.4 kPa, respectively[30]. Therefore, selecting the appropriate cellular source can adjust the flexibility of EVs.

The flexibility of EVs gives them excellent tumor penetration. As early as 2016, Ma et al.[206] found that the novel penetration of drug-carrying tumor exosomes into tumor tissues was related to their deformability. The softness of EVs can also be adjusted by changing the flexibility of the extracellular matrix. Liang et al.[125] demonstrated a method to adjust the flexibility of EVs by culturing tumor cells in elastic soft fibrin gels (90 Pa). The resulting exosomes were found to be softer, with Young's moduli of 1 kPa compared to 3 kPa for those cultured on rigid two-dimensional plastics. This indicated that the method of obtaining exosomes from elastic gels could effectively reduce their

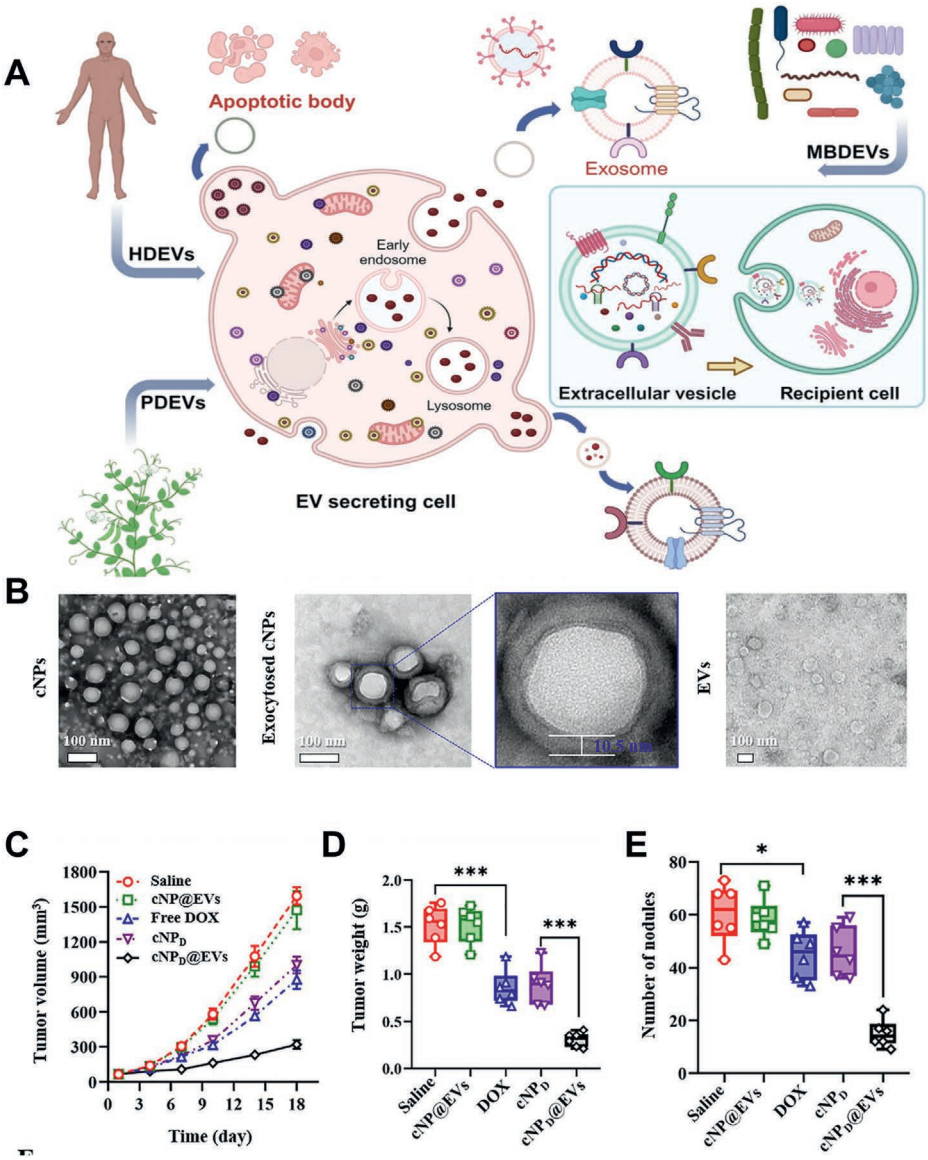

Figure 7 The inherent flexibility and bioengineering of EVs confer superior tumor-targeting and penetration capabilities. (A) Visual description of the types and sources of EVs. Reprinted with the permission from Ref. 204. Copyright © 2024 Springer Nature. (B) TEM image of EVs after "cell travel". Tumor growth curve (C) and tumor weight (D) after treatment for each group. (E) Pulmonary metastatic nodules in lung tissue after different treatments. Reprinted with the permission from Ref. 126. Copyright © 2023 American Chemical Society.

stiffness. According to proteome analysis, the authors concluded that the reduction in exosome stiffness was mediated by the regulation of cytospin-A, as the low expression of cytospin-A in cells was responsible for the decreased exosome stiffness. The research team encapsulated doxorubicin in stiff and soft exosomes, respectively. Compared with stiff drug-carrying exosomes (3 kPa), soft drug-carrying vesicles (1 kPa) demonstrated superior antitumor efficacy. After injection into H22 tumor-bearing mice, the stiff drug-carrying exosomes achieved 72.6% tumor inhibition. However, the soft ones achieved 91.5% tumor shrinkage. By adjusting exosome stiffness with Jasplakinolide and latA treatment, it can be concluded that mechanical softness promoted EVs penetration in tumors. In short, soft drug-carrying exosomes have a better effect on tumor inhibition, which is caused by two factors. On the one hand, macrophages tend to phagocytose stiff particles, which leads to the loss of drugs in the blood circulation, so the soft drug carrier can be retained more effectively. On the other hand, tumor cells have a propensity to internalize soft particles, which enhances the delivery efficiency of soft DDS.

4.4.2. Adjusting the tissue penetration properties by modulating the Young's modulus of EVs

The unique properties of EVs enable them to effectively penetrate the BBB, a significant obstacle in brain tumor treatment. Research indicated that EVs could cross the BBB through transcytosis. In a study using a zebrafish model, EVs isolated from brain-seeking cells exhibited a lipid bilayer structure and a mode size of 158.5 ± 6.0 nm. Live imaging revealed that these EVs were taken up by various cells within the brain parenchyma, demonstrating

their capacity to traverse the BBB. Furthermore, the movement of EV-containing endocytic vesicles within endothelial cells suggested a process of transcytosis. As the stiffness of vesicles is known to influence transcytosis efficiency, it is plausible that the flexibility of EVs contributes to their ability to penetrate the BBB, although research in this area remains limited. Early studies, such as one by Ma et al.[206], have established a correlation between the deformability of drug-carrying tumor exosomes and their ability to penetrate tumor tissues.

Nucleated EVs, produced by a process metaphorically termed "cell travel", exhibit excellent properties in the field of drug delivery. Cationic polymer nanoparticles (cNPs) could be released from the cell in an EV-coated form after endocytosis, a mechanism that can be expressed as "cell travel"[207]. Shang's work[126] revealed that the NPs obtained through this process exhibited good tumor permeability (Fig. 7B−E). Doxorubicin (DOX), a potent anticancer drug, could be preloaded into cNPs, which could then be enveloped by EVs through cell travel. Fluorescence images showed that EV-coated cNPs achieved significant tumor penetration compared with free cNPs. The amount of EV-coated cNPs delivered to tumor spheres was about 2.31 times that of free DOX-treated tumor spheres, a process facilitated by the transfer properties of EVs. Furthermore, in 4T1 tumor-bearing BALB/c mice, treatment with EV-coated cNPs resulted in a tumor weight reduction to approximately 0.31 g, which was only 20.1% of that in the saline group, 35.7% of that in the Dox group, and 34.5% of that in the cNPs-DOX group. At the same time, EV-coated cNPs could effectively inhibit lung metastasis of tumors. The number of pulmonary metastasis nodules was only about 15 per lung tissue, which was 24.8% of that in the saline group, 33.5% of that in the DOX treatment group, and 32.6% of that in the cNPs-Dox treatment group. This approach offers the flexibility to adjust the stiffness of EVs by modulating the composition of the NPs. In addition, increasing the cholesterol content of EVs can promote their deformation and contact with the target cell membrane, thus promoting membrane fusion[127].

In summary, the flexibility of EVs plays a crucial role in their effectiveness as DDS, influencing their ability to navigate biological barriers and penetrate target tissues. This tunable property allows for the optimization of EVs to better suit specific therapeutic needs, potentially enhancing their efficacy in drug delivery and tumor targeting. The ability to fine-tune the mechanical properties of EVs, in conjunction with their natural biological properties, positions them as a soft and potent tool in the arsenal against cancer.

4.5. Liposomes

Liposomes were first discovered by British hematologist Dr. Alec D. Bangham and his collaborators at the Babraham Institute, University of Cambridge, in the 1960s, with the first report published in 1964. Liposomes are defined as closed phospholipid bilayer systems[208]. Their unique bilayer structure allows for the encapsulation of drugs with different solubilities: hydrophilic molecules in the inner aqueous core, hydrophobic molecules entering the lipid bilayer, and amphiphilic molecules residing at the water/lipid bilayer interface[209]. Liposomes are considered powerful DDS due to their structural versatility, biocompatibility, biodegradability, non-toxicity, and non-immunogenicity[210]. For liposomes, the main means to regulate their mechanical flexibility lies in precisely designing the composition of the phospholipid bilayer or core, thereby achieving the control of Young's modulus from tens of kPa to hundreds of MPa.

4.5.1. Liposomes as artificial cells and mechanical signal simulation

The fluidity of liposomes can enhance the multivalent interactions of membranes. A recent study prepared lipid vesicles coupled with immuno-stimulatory antibodies to function as aAPCs[122]. FRAP experiments showed that due to the high fluidity of lipid membranes, aAPCs possess a higher diffusion rate, indicating that a greater number of ligands can diffuse to the regions where immune synapses are formed. Under the stimulation of aAPCs, the secretion of IFN-γ, TNF-α, IL-10, and IL-2 by PBMCs increased 28, 7, 17, and 9.6 times, respectively. This underscores the significance of liposomal fluidity in modulating immune responses and the potential of liposomes in advanced drug delivery applications. Therefore, liposomes can also exert therapeutic effects by transmitting mechanical signals.

4.5.2. Adjusting the flexibility of liposomes by changing the composition

The flexibility of liposomes is indeed intricately tied to their lipid composition, allowing for the modulation of their mechanical properties through the selection of specific phospholipids. The main component of liposomes is glycerophospholipids, which are amphiphilic lipids consisting of a glycerol molecule bound to a phosphate group and two saturated or unsaturated fatty acid chains[117]. The length and saturation of fatty acid chains, the backbone of phospholipids, and the heterogeneity significantly influence the flexibility of liposomes. For instance, phospholipids with stronger hydrogen bonding abilities have a higher Young's modulus. Compared to DPPC-based liposomes (116 MPa), Sphingosine-based liposomes, which can easily form hydrogen bonds, displayed a significantly higher Young's modulus (188 MPa). The number of carbon atoms in the saturated acyl chain of sphingomyelin (SM) also affects the Young's modulus. For example, the Young's modulus of C24:0-SM (24 carbon atoms) was significantly larger than that of C16:0-SM (16 carbon atoms). The heterogeneity induced by the codispersion of SM molecules with different acyl chain lengths has a significant effect on the mechanical properties of lipid membranes, manifested by a decrease in Young's modulus. When C24:0-SM was mixed with C16:0-SM in a ratio of 1 to 1, the resulting liposomes exhibited a reduced Young's modulus (214−287 MPa) compared to pure C24:0-SM liposomes (262 $\pm$ 47 or 471 $\pm$ 181 MPa).

Additionally, the presence of unsaturated chains reduced Young's modulus. C24:1-SM, containing one additional unsaturated bond on the acyl chain than C24:0-SM, showed a significantly reduced Young's modulus when mixed with C24:0-SM at a molar ratio of 5: 95 (80 $\pm$ 24 MPa). It indicated that a small amount of unsaturated lipids can significantly change the Young's modulus of liposomes[211]. On the whole, by changing the phospholipid components, the stiffness of liposomes can be adjusted to optimize their performance in drug delivery, particularly in tumor treatment (Fig. 8)[62]. Studies have shown that liposomes with moderate stiffness (19.9 MPa) exhibited excellent penetration in BxPC-3-HPSC tumor xenografts and uptake by pancreatic adenocarcinoma cells (BxPC-3) and human pancreatic stellate cells (HPSC), resulting in the most effective tumor inhibition effect[62]. This highlights the importance of liposomal flexibility in enhancing the efficacy of DDS.

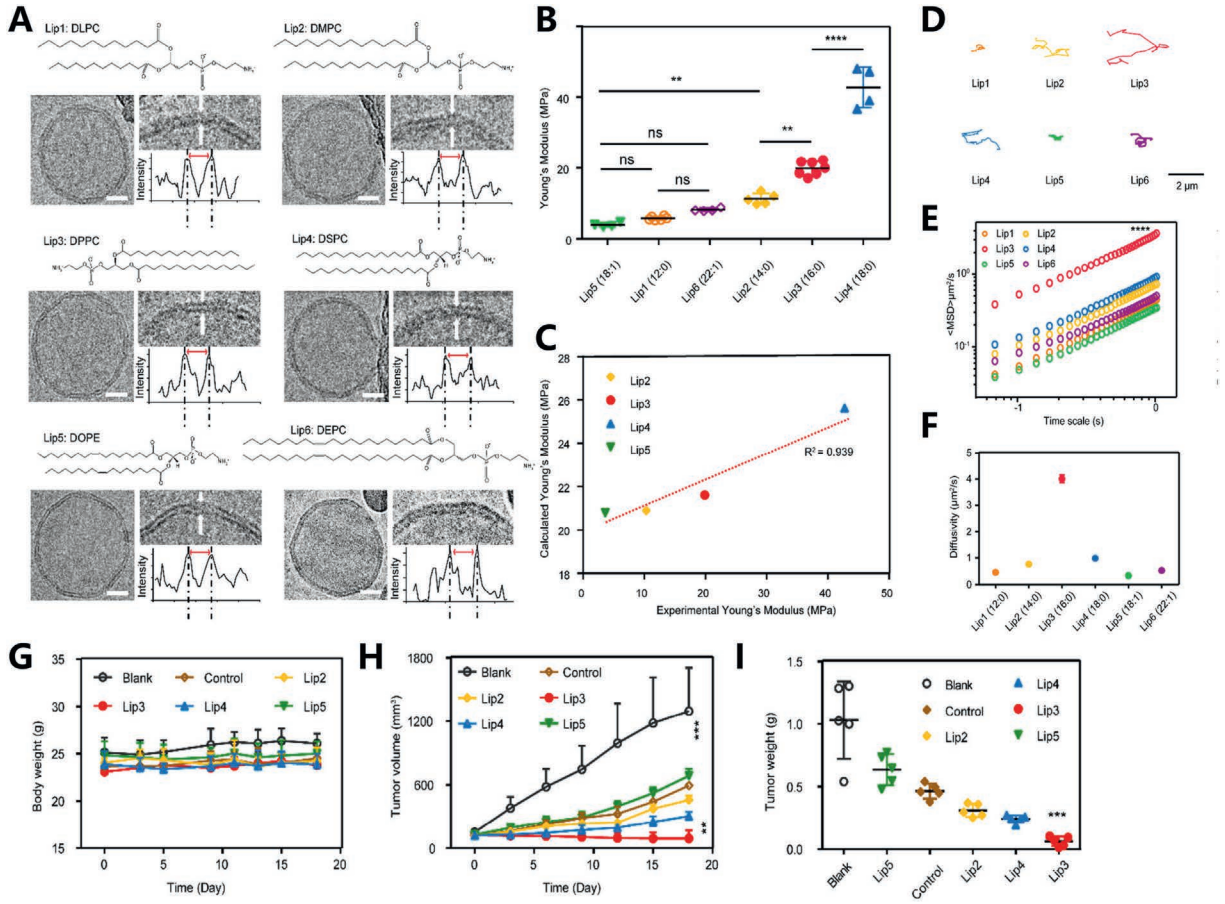

Figure 8 The optimization of liposomal stiffness through precise compositional control, can maximize tumor penetration and therapeutic outcomes. (A) Cryogenic transmission electron microscopy (cryo-TEM) images of liposomes. (B) Young's modulus of liposomes tested in solution using AFM. (C) Correlation between experimental Young's modulus data and calculated Young's modulus values. (D) The representative trajectory of the diffusion of liposomes in extracellular matrix (ECM), simulated in 1 s. (E) The logarithmic distribution of the effective diffusion coefficient (Deff) values of a single liposome in the ECM at 1 s. (F) The diffusion rate of liposomes at 1 s in a simulated ECM. (G) Weight changes of nude mice with BxPC-3-HPSC tumor treated with different formulations. (H) Tumor volume in different treatment groups. (I) Weight of the BxPC-3-HPSC tumor at the end of treatment. Reprinted with the permission from Ref. 62. Copyright © 2019 American Chemical Society.

4.5.3. Adjusting the flexibility of liposomes by adding ingredients

The flexibility of the liposomes can also be adjusted by adding ingredients. Transfersomes can be used as modified liposomes with soft and elastic properties. Trotta et al.[24] developed deformable liposomes by adding surfactants and used them to improve the transdermal delivery of methotrexate. These modified liposomes exhibited high deformability and elasticity, allowing them to pass through barriers with pores smaller than approximately three times their own diameter. *In vitro* studies have shown that the skin penetration of methotrexate in deformable liposomes was 3−4 times that of the rigid ones in a pig ear skin model[24].

As another special class of liposome proposed by Touitou in 2000, ethosomes containing ethanol possessed soft and deformable characteristics, making them easier to penetrate into the deeper layers of the skin[119]. Fu et al.[212] prepared a special ethosome for transdermal delivery of thymosin β-4 (Tβ-4), a protein that is poorly absorbed through oral or transdermal administration alone. This ethosome, containing soya PC, sodium deoxycholate, and cholesterol, exhibited higher transdermal efficiency compared with free drugs. Ethosomes can also be combined with other substances to further improve transdermal efficiency. Yang et al.[101] prepared a novel hyaluronic acid (HA) and galactose-chitosan (GC) modified ethosome (Eth-HA-GC) by a layer-by-layer self-assembly technique, which demonstrated superior drug retention in skin tissue compared to control formulations. The galactose group was utilized to target DCs. Then, Eth-HA-GC was loaded in SF nanofibrous mats. Eth-loaded SF nanofibrous mats (ESNFM) showed a good transdermal delivery effect. *In vitro* experiments showed that the amount of drug retention in skin tissue of the ESNFM group was significantly higher than that of the SF group.

Following the innovations of transfersomes (TEL) and ethosomes, a new generation of nanovesicle carriers have been developed, including transethosomes and glycerosomes. Song et al.[123] proposed the concept of TEL. TEL, a hybrid of transfersomes and ethosomes, are created by integrating edge activators or permeation enhancers with ethanol. For example, TEL were prepared by adding the edge activator Tween 80, sodium taurocholate and oleic acid (0.53%, *w*/*w*) to ethosomes containing 30% ethanol. Compared with traditional liposomes and ethosomes, TEL showed higher flexibility and skin deposition[123]. In a

recent study, TEL was used to achieve transdermal delivery of ginger extract (GE). The skin deposition of GE TEL hydrogel reached 20.87%, while the skin deposition of free GE HPMC hydrogel and GE solution were 10.25% and 5.81%, respectively[124].

Glycerosomes (GS), prepared by adding 10%−30% *v/v* glycerol to DMPC liposomes, also enhanced transdermal delivery. The content of glycerol measured by extrusion method was positively correlated with the deformability of GS. *In vitro* experiments using diclofenac sodium salt as a model drug showed that the transdermal delivery amount using 30%, 20%, and 10% glycerol was 5.5, 3.7, and 2.5 times higher than that of liposomes, respectively[120,121].

4.5.4. Adjusting the flexibility of liposomes by adding an inner core

Another approach to modulate liposomal stiffness involves incorporating a poly(lactic-co-glycolic acid) (PLGA) core into lipid vesicles. As the size of the PLGA core increased, the water content in the liposomes decreased, leading to higher rigidity[213]. Liposomes with a 120 nm diameter PLGA core and moderate stiffness (712 kPa) showed the best ability to penetrate mucus and a moderate capacity for endocytosis and exocytosis in orally-delivered NPs for the treatment of liver fibrosis, indicating that its targeting efficiency was higher than that of soft particles (85 kPa) but lower than that of rigid particles (2118 kPa)[12]. This rigid core composition of liposomes was not limited to PLGA. The rigidity of the liposomes can also be regulated by a crosslinking strategy using cGAMP and 5′-GMP with different concentrations of $Zn(NO_3)_2$ in the core. With the concentration of Zn^{2+} from 0 to 10 mmol/L, the Young's modulus of the obtained liposomes increased from 15 to 149 MPa[74]. Besides, adding sodium alginate and a crosslinker can adjust the rigidity of liposomes. The Young's modulus of the DOPC liposomes with an aqueous core is 45 kPa, and that of the liposomes with only sodium alginate in the core was 1.6 MPa. With the increase of crosslinker $CaCl_2$ concentration, Young's modulus increased from 1.6 to 19 MPa. In 4T1 breast tumor models, the lower the liposomal stiffness, the better the uptake effect[118].

In summary, the flexibility of liposomal vesicles plays a significant role in both *in vivo* and transdermal drug delivery, influencing the efficacy and penetration of therapeutic agents.

4.6. Other platforms

While the principle of tuning flexibility has been extensively discussed in the context of coacervates, gels, Pickering emulsions, EVs, and liposomes, its application is by no means limited to these platforms. In fact, several conventional and emerging platforms, though diverse in composition and design, also embody the essential features of DDS, including structural flexibility, functional adaptability, and traceable delivery mechanisms. Among conventional carriers, polymeric micelles have long been utilized for solubilizing poorly water-soluble drugs, offering favorable pharmacokinetics and tunable release[214]. Likewise, self-assembling peptide-based NPs can provide a modular approach with precise sequence design, excellent biocompatibility, and responsiveness to specific physiological cues[215]. These systems, although well established, remain integral to the mechanically tuned DDS framework by virtue of their design controllability and functional flexibility.

In recent years, artificial cell-based systems have gained attention as next-generation mechanically tuned DDS platforms[216]. Notably, giant unilamellar vesicles (GUVs), a kind of cell-sized vesicle capable of encapsulating proteins, gene circuits, or synthetic biology components, can offer programmable, stimuli-responsive delivery with high biomimicry[217,218]. Drawing inspiration from red blood cells (RBCs), GUVs have been engineered to mimic RBC deformability, membrane features, and immune evasion[219,220]. Advanced RBC-mimetic designs further integrate GUVs with membranes from platelets, tumor cells, or bacteria to enhance targeting, circulation, and immunomodulation[221-224]. Another promising biomimetic strategy involves enucleated cells such as Cargocytes, derived from mesenchymal stromal cells[114,225]. These carriers can eliminate the stiff nucleus with greatly improved deformability while preserving key functions like chemotaxis and protein secretion. As such, they bridge the gap between cellular navigation and nanoparticle-scale tissue penetration, uniquely fitting the soft DDS model. In the realm of synthetic platforms, several vesicular systems can also expand the soft DDS toolbox: 1) Polymersomes, with soft membrane thickness and environmental responsiveness, provide robust structural control[226,227]. 2) Proteinosomes, constructed from protein−polymer hybrids, achieve bioresponsive delivery through light or redox activation[228]. 3) Hybrid lipid−polymer vesicles combine membrane proteins with durable polymer matrices, balancing biological activity with release control[229,230]. Beyond these, advanced structures such as multicompartment vesicles (*e.g.*, vesosomes)[231] can enable stepwise or synergistic delivery, while protein nanocages (*e.g.*, ferritin)[232,233] and DNA nanostructures can offer genetically encoded, logic-gated release mechanisms that support precise, biomarker-responsive therapies[234,235].

Together, these platforms extend the mechanically tuned DDS paradigm by integrating active design, mechanistic delivery control, and adaptive functionality, thus broadening the classification framework and opening new opportunities for clinical translation.

5. Clinical application and limitations

DDS can be engineered to dynamically adapt to physiological environments, enhancing therapeutic precision through responsive material properties. By converting mechanical or environmental stimuli into controlled drug release, DDS can improve bioavailability and tissue targeting while minimizing systemic toxicity. Representative platforms, including liposomes, EVs, coacervates, hydrogels, and Pickering emulsions, can exploit system stiffness in distinct ways to navigate biological barriers and enable localized drug delivery. This section outlines the translational potential and key limitations of these systems, highlighting strategies for clinical advancement (Table 3).

(1) Coacervates, formed *via* LLPS, represent a soft class of biomimetic DDS. Their dynamic fluidity, compartmentalized architecture, and compositional adaptability can offer advantages in gastrointestinal retention (>24 h in inflamed colonic tissue)[57] and cytosolic transfection[236]. Preclinical studies show promise in treating inflammatory bowel disease, diabetic wounds, tumor embolization, and cartilage repair. For example, HB-EGF-loaded coacervates accelerated diabetic wound healing[237], and BMP-2-loaded coacervates aided cartilage regeneration[238]. Yet, no

Table 3 Recent clinical trials focusing on mechanically tuned DDS were extracted from clinicaltrials.gov.

Trial identifier	Trial phase	Condition	Trial purpose or intervention	Start date
NCT04908748	Phase II	Soft tissue injuries	Esflurbiprofen hydrogel patch	2021-05-20
NCT04892706	Phase II	Acne vulgaris	IDP-126 Gel *vs.* IDP-126 vehicle Gel *vs.* Epiduo® Forte Gel (0.3% Adapalene/2.5% BPO)	2021-06-11
NCT04983849	Phase IV	Periodontitis	Metronidazole hydrogel 25%	2021-07-07
NCT05005845	Phase II	Neurofibromatosis 1 and cutaneous neurofibromas	Two concentrations of NFX-179 topical gel (0.5% *vs.* 1.5%)	2021-09-20
NCT05298917	Not applicable	Cornea	Influence of silicone hydrogel extended contact lens wear on corneal sensitivity	2022-04-01
NCT05394662	Phase III	Intrauterine adhesion	Intrauterine instillation of Juveena post-TCGP *vs.* standard care (TCGP only).	2022-08-11
NCT06373757	Not applicable	Periodontal intrabony defects	Nano-hydroxyapatite/Chitosan hydrogel	2023-03-01
NCT05745220	Not applicable	Cornea	Corneal sensitivity in silicone hydrogel contact lens wear	2023-04-08
NCT05411484	Phase II	Wounds and injury/ wound healing assessment	Laser assisted drug delivery of NanoDOX® hydrogel (1% doxycycline)	2023-11-29
NCT06715345	Not applicable	Degenerative lumbar diseases	Recombinant human bone morphogenetic protein-2 + β-tricalcium phosphate/hydrogel (NOVOSIS PUTTY)	2024-03-06
NCT06369987	Not applicable	Presbyopia	To evaluate logMAR visual acuity with silicone hydrogel multifocal lenses (Delefilcon A, Senofilcon A)	2024-04-25
NCT06469242	Not applicable	Presbyopia	Two frequent replacement silicone hydrogel multifocal contact lenses	2024-07-18
NCT06748404	Phase II	Immunotherapy-related pruritus	A topical gel containing strontium (TriCalm Hydrogel®)	2025-01-31
NCT06634719	Not applicable	Heavy menstrual bleeding	Evaluate the Juveena Hydrogel system, a single-use liquid-to-gel device for intrauterine tamponade.	2025-02-01
NCT06897215	Not applicable	Oral mucositis due to radiation (head and neck cancer)	Hyaluronic acid hydrogel (Gelclair)	2025-05-01 (estimated)
NCT06839222	Not applicable	Knee osteoarthritis (Knee OA)	Hydrogel OA 2% (ultra-pure bovine gelatin) *vs.* Hyaluronic acid (Durolane),	2025-06 (estimated)
NCT07060495	Phase III	Postoperative pain (tonsillectomy procedures)	RADA16 hydrogel (PuraStat®, PuraGel®, or PuraSinus®)	2025-08-01 (estimated)
NCT06957197	Phase III	Socket preservation after tooth extraction	Xenograft with hydrogel *vs.* Xenograft alone	2025-09-22 (estimated)

Recent observational and clinical trials of extracellular vesicles

Trial identifier	Trial phase	Condition	Trial purpose or intervention	Start date
NCT04892433	Observational	CAR T cell therapy	EV-derived miRNAs *vs.* clinical outcomes	2021-05-14
NCT05078385	Phase I	Deep second-degree burns	Bone marrow MSC-EVs therapy (topical)	2021-12-22
NCT05228899	Phase I/II	Long COVID (6 weeks −24 months)	IV Zofin (MSC-EVs therapy)	2022-04-14
NCT04815213	Phase I	Premature Ovarian failure	Autologous bone marrow MSC injection	2022-01-01
NCT06813027	Phase I	Vitiligo	Repeated perilesional injections of UCMSCs secretomes	2023-01-01
NCT05774509	Phase I	Heart failure with reduced ejection fraction	IV cardiovascular progenitor cell EVs (SECRET-HF)	2023-05-31
NCT06539273	Phase III	Androgenetic Alopecia	IV foreskin-derived mesenchymal stromal cells derived exosome	2024-01-01
NCT06334653	Not applicable	Healthy volunteers/only energy metabolism	Exercise-regulated organ crosstalk, influence of IL-6 (EVEX)	2024-04-09
NCT06850935	Not applicable	Skin quality	Evaluate skincare effects of *Centella asiatica* EV-based formulation	2024-09-04
NCT06825884	Phase I	Diabetic foot ulcers	Perilesional EVs injection	2024-12-01
NCT06865924	Not applicable	Primary sclerosing cholangitis	Use assembloids as *in vitro* models to test new pharmacological approaches	2024-12-01

Table 3 (*continued*)

Trial identifier	Trial phase	Condition	Trial purpose or intervention	Start date
NCT06869135	Observational	Neurodegenerative diseases	Diagnosis of neurodegenerative diseases based on saliva and sEV biochemical profiling	2025-01-24
NCT06546085	Not applicable	Type 2 diabetes/obesity	EVs in type 2 diabetes−related cardiovascular disease: Impact of exercise on vascular and metabolic effects	2025-02-10
NCT06620809	Phase I	Neuromyelitis optica spectrum disorder	Intrathecal neural stem cell EVs (NouvSoma001)	2025-03-28
NCT06985121	Not applicable	Scalp health	(Base formula plus IGF-1 and FGF-7) *vs.* (base formula plus *Centella asiatica* extracellular vesicles) *vs.* (base formula plus *Centella asiatica* extracellular vesicles, IGF-1 & FGF-7)	2025-04-08
NCT06706102	Phase IV	Immune effector cell associated neurotoxicity syndrome	Temporal characterization of EVs during cellular therapy using CAR-T cells and during the occurrence of immune Effector cell-associated Neurotoxicity Syndrome	2025-07-02
NCT06612710	Phase I	Ischemic stroke	IV neural stem cell EVs (NouvSoma001)	2025-07-30 (estimated)
NCT06995625	Phase I	Acute ischemic stroke (AIS)	Allogeneic Wharton's jelly-mesenchymal stem cell-derived EVs (SNE-101)	2025-08-01 (estimated)
Recent observational and clinical trials of liposomes				
Trial identifier	Trial phase	Condition	Trial purpose or intervention	Start date
NCT04727853	Phase II	Small cell lung cancer (SCLC)	IV irinotecan liposome with SCLC who have progressed after platinum-based first-line therapy	2021-03-01
NCT06527729	Early phase I	Alopecia Areata	Sildenafil-loaded liposomes/minoxidil gel	2021-07-01
NCT06098599	Phase I	Advanced breast cancer	Doxorubicin hydrochloride liposome injection	2022-05-17
NCT05383352	Phase I	Metastatic pancreatic adenocarcinoma	Compare Onivyde manufactured at two different production sites	2022-05-30
NCT05739630	Phase II/III	Acute leukemia	Bioequivalence of amphotericin B liposome for injection	2023-01-01
NCT06806410	Phase IV	Supraclavicular nerve blocks for hand and wrist surgery	Liposomal bupivacaine/Dexamethasone	2023-05-01
NCT05913921	Phase I	Bioequivalence	IV amphotericin B liposome	2023-06-02
NCT05763667	Phase III	Endometrial cancer	Liposomal bupivacaine in endometrial cancer surgery	2024-01-01
NCT06867939	Not applicable	Inflamatory bowel disease	Liposomal curcumin	2024-05-05
NCT06233591	Phase I	Oral lichen planus	LP-10 (liposomal Tacrolimus)	2024-07-01
NCT06771388	Not applicable	Skin diseases	Liposomal collagen drink/To assess avance QQ collagen product on skin condition improvement	2024-11-01
NCT06392191	Not applicable	Thoracic surgery	Liposomal bupivacaine *vs.* conventional bupivacaine/dexamethasone	2024-11-10
NCT06763029	Phase II	Colorectal cancer metastatic	Irinotecan liposomes combined with cetuximab + vermofenib	2025-02-26
NCT06876636	Not applicable	Breast cancer metastatic	Zoledronic acid + liposomal doxorubicin + cyclophosphamide	2025-03-10
NCT06980493	Phase I	Tinea capitis	Amphotericin B liposome (Ambisome®)	2025-04-01
NCT06827717	Phase II	Ewing sarcoma	Irinotecan liposome (II) + temozolomide + fluzoparib	2025-04-15
NCT06972680	Observational	Shoulder Arthroscopy	Determine the optimal volume of 0.5% liposomal bupivacaine for single-injection interscalene brachial plexus block.	2025-05-01
NCT07020468	Phase IV	Colorectal cancer (CRC)	Oxaliplatin + Irinotecan Liposome + 5-FU/LV (NALIRIFOX)	2025-05-15
NCT06995352	Phase IV	Moderate-to-severely painful ankle surgery	Liposomal bupivacaine *vs.* continuous peripheral nerve blocks (Ankle)	2025-06-23
NCT06981637	Phase II	Advanced soft tissue sarcoma	Pegylated liposomal doxorubicin	2025-07-01 (estimated)

(*continued on next page*)

Table 3 (*continued*)

Trial identifier	Trial phase	Condition	Trial purpose or intervention	Start date
NCT07051785	Phase II	Colorectal cancer (CRC)	(Fruquintinib + Irinotecan Liposome + Capecitabine) *vs.* (Bevacizumab + Irinotecan Liposome + Capecitabine)	2025-07-07 (estimated)
NCT05411237	Phase III	AIDS-related Kaposi Sarcoma	Pegylated liposomal doxorubicin *vs.* Paclitaxel	2025-09-15 (estimated)

MSC, mesenchymal stem cell; IV, intravenous; UCMSC, umbilical cord mesenchymal cells; ATG, anti-thymocyte globulin.

coacervate-based formulation has entered clinical trials. Translational hurdles include dilution-induced instability and batch variability. Current solutions focus on covalent crosslinking, core-shell encapsulation, multicomponent co-assembly, and membrane mimicry[239-241]. Microfluidic fabrication could enhance scalability and uniformity[242], while improved understanding of entropy-driven assembly will support clinical translation.

(2) Hydrogels exemplify DDS softness through their ECM-like networks, high water content, and tunable mechanics. Clinically approved hydrogels (*e.g.*, DermiSphere hDRT for wounds, SpaceOAR for radioprotection, Bulkamid for incontinence) demonstrate their medical utility in tissue repair and protection. Innovations, such as brain-penetrating glioblastoma gels and thermo-responsive biosensors, have expanded their scope. Mechanical compliance is mainly achieved by modulating crosslinking density, allowing compatibility with dynamic tissues like the lung or intestine. However, clinical translation remains constrained by several challenges: 1) Mechanical limitations—high water content improves biocompatibility but weakens structural stability, while overly stiff matrices may induce inflammation or impair cellular mechanotransduction; 2) Manufacturing scalability—batch variability in complex formulations hampers reproducibility and regulatory approval; 3) Implantation risks—long-term complications such as calcification and unpredictable immune responses persist[243]. To overcome these barriers, multidisciplinary strategies have been adopted, including AI-assisted microfluidic printing, supercritical CO_2 sterilization[244], and organoid-based predictive models. As smart systems like enzyme-responsive or conductive neural hydrogels move toward clinical trials, hydrogels are evolving from inert carriers to dynamic, biointeractive platforms. Their design principles, particularly in mechanical tuning and tissue compliance, can offer important references for other DDS aiming to balance biofunctionality with structural integrity.

(3) Pickering emulsions are stabilized by solid particles at oil-water interfaces, offering deformable and mechanically stable carriers with tunable interfacial properties. Their inherent flexibility enables deep tissue penetration and mucosal adhesion, making them ideal for tumor-targeted therapies and vaccine delivery. PLGA-stabilized Pickering emulsions have shown mechano-responsive behavior that boosts antigen presentation and immune activation[245]. Despite promising preclinical data, their clinical translation is hindered by: 1) Material instability—susceptibility to phase separation, enzymatic degradation, and loss of interfacial cohesion; 2) Scale-up difficulties—low-throughput microfluidics and formulation instability during homogenization reduce production efficiency; 3) Immunogenicity—fine-tuning surface charge and particle hydrophobicity remains challenging. Emerging solutions include particle surface modification[246], jetting-based scale-up technologies (JetALL)[247] and hierarchical structures like Pickering double emulsions (W/O/W or O/W/O)[248], which can enhance both biocompatibility and modular design. As programmable emulsions, Pickering systems demonstrate how DDS can combine structural rigidity with interfacial adaptability.

(4) EVs are nanoscale carriers characterized by intrinsic membrane integrity, immune evasion, and organotropism. Their cargo and targeting stem from parental cell origin, and their function can be enhanced through bioengineering such as ligand addition or electroporation. EVs can cross biological barriers, enabling gene silencing, immune modulation, and microenvironmental remodeling. Several candidates are in phase I/II clinical trials, such as in diabetic wound healing (NCT06825884), ischemic stroke (NCT06612710), myocardial repair (NCT05774509), and autoimmune disorders (NCT06620809). Despite this progress, key translational hurdles remain: 1) Low yield and poorly scalable isolation techniques limit production consistency; 2) Delivery efficiency and programmable cargo loading are constrained by the need to preserve vesicle integrity; 3) Regulatory uncertainty persists due to EVs' hybrid identity as both biologics and nanocarriers. Recent innovations, such as bioreactor-enabled scalable manufacturing[249,250], AI-assisted multi-omics optimization, and membrane-responsive cargo release, are addressing these limitations[251,252]. Notably, EVs represent a distinctive mode of biologically encoded flexibility, offering a mechanistic and functional sophistication that is challenging to reproduce synthetically.

(5) Liposomes are among the most clinically validated DDS, with approved products such as Doxil, Onivyde, and AmBisome. Their tunable lipid structure enables control over circulation, uptake, and permeability. Despite decades of clinical application, several bottlenecks persist, such as poor intratumoral release (*e.g.*, SPI-077[253,254]), limited success in stimuli-responsive delivery (*e.g.*, ThermoDox®)[255], and a continued reliance on passive targeting that can reduce efficacy. Most formulations are reformulated legacy drugs, with mRNA-LNP success not yet replicated for small molecules. Advances now mainly focus on hybrid co-delivery systems, dynamic release mechanisms, and organoid-based predictive models. The

translational trajectory of liposomes illustrates a key lesson for future mechanically tuned DDS: clinical success hinges not on isolated parameters, but on the synergy of structural programmability and spatiotemporal control. This principle increasingly informs the design of next-generation platforms, including biomimetic, immune-modulatory, and multi-responsive liposomal carriers.

6. Conclusion and perspectives

Mechanically tuned DDS have moved beyond simply deformable carriers to become adjustable and bioresponsive platforms capable of sensing, adapting, and responding to complex physiological environments. Their structural tunability, biomechanical compatibility, and programmable functionality have enabled promising advances in cancer therapy, wound healing, and neurological disorders. However, clinical translation remains limited, not by the concept of "softness" itself, but by its insufficient integration with material intelligence, scalable manufacturing, and application-specific design.

To bridge this gap, three key development directions should be emphasized:

1) Material intelligence: next-generation DDS should shift from passive softness to active adaptability, either by leveraging bioresponsive materials for context-aware release, dynamic stiffening, and biosignal integration. This requires embedding logic-responsive modules and real-time feedback elements into their design.
2) Manufacturing convergence: lab-scale innovations must be transformed into clinically viable products *via* standardized flexibility metrics, AI-assisted formulation, and GMP-compatible microfluidic systems. Regulatory frameworks should evolve to address DDS-specific challenges in stability, release control, and batch variability.
3) Clinical application focus: mechanically tuned DDS will have great impact where conventional systems fail, such as in immunomodulation, BBB penetration, and dynamic remodeling tissues. Here, their adaptability provides unmatched advantages in precision, efficacy, and patient-specific customization.

The future of DDS lies not merely in being soft or stiff, but in learning to flex intelligently, creating closed-loop systems that can dynamically adapt to disease states and therapeutic demands. This vision will require interdisciplinary collaboration across materials science, synthetic biology, clinical pharmacology, and digital medicine.

Acknowledgments

This research was supported by Hubei Provincial Health Commission Project (No. ZY2025Q028, China) and National Natural Science Foundation of China (No. 82373816).

Author contributions

Conglian Yang and Zhiping Zhang conceived and designed the project. Kangyuan Qi and Shasha Zhang drafted and revised the manuscript. Xinying Bi gave some critical suggestions to the manuscript. All authors read and approved the final manuscript.

Conflicts of interest

The authors declare no conflicts of interest.

References

1. Zhang Y, Habibovic P. Delivering mechanical stimulation to cells: state of the art in materials and devices design. *Adv Mater* 2022;**34**: e2110267.
2. Xiao BL. Mechanisms of mechanotransduction and physiological roles of PIEZO channels. *Nat Rev Mol Cell Biol* 2024;**25**:886−903.
3. Ping YQ, Xiao P, Yang F, Zhao RJ, Guo SC, Yan X, et al. Structural basis for the tethered peptide activation of adhesion GPCRs. *Nature* 2022;**604**:763−70.
4. Yao WD, Jiang DM, Fan QM, Weng YY, Xie XZ, Zheng S, et al. Biomechanical forces and force-triggered drug delivery in tumor neovascularization. *Biomed Pharmacother* 2024;**171**:116117.
5. Li N, Zhang XY, Zhou J, Li W, Shu XY, Wu Y, et al. Multiscale biomechanics and mechanotransduction from liver fibrosis to cancer. *Adv Drug Deliv Rev* 2022;**188**:114448.
6. Lei K, Kurum A, Tang L. Mechanical immunoengineering of T cells for therapeutic applications. *Acc Chem Res* 2020;**53**:2777−90.
7. Hu YR, Li HY, Wang WX, Sun F, Wu CY, Chen W, et al. Molecular force imaging reveals that integrin-dependent mechanical checkpoint regulates Fcγ-receptor-mediated phagocytosis in macrophages. *Nano Lett* 2023;**23**:5562−72.
8. Bakalar MH, Joffe AM, Schmid EM, Son S, Podolski M, Fletcher DA. Size-dependent segregation controls macrophage phagocytosis of antibody-opsonized targets. *Cell* 2018;**174**: 131−42.e13.
9. Freeman SA, Goyette J, Furuya W, Woods EC, Bertozzi CR, Bergmeier W, et al. Integrins form an expanding diffusional barrier that coordinates phagocytosis. *Cell* 2016;**164**:128−40.
10. Ostrowski PP, Freeman SA, Fairn G, Grinstein S. Dynamic podosome-like structures in nascent phagosomes are coordinated by phosphoinositides. *Dev Cell* 2019;**50**:397−410.e3.
11. Jiang XH, Xu S, Miao YQ, Huang K, Wang BQ, Ding B, et al. Curvature-mediated rapid extravasation and penetration of nanoparticles against interstitial fluid pressure for improved drug delivery. *Proc Natl Acad Sci U S A* 2024;**121**:e2319880121.
12. Yu YL, Xing LY, Li L, Wu JW, He JJ, Huang Y. Coordination of rigidity modulation and targeting ligand modification on orally-delivered nanoparticles for the treatment of liver fibrosis. *J Control Release* 2022;**341**:215−26.
13. Majedi FS, Hasani-Sadrabadi MM, Thauland TJ, Li S, Bouchard LS, Butte MJ. Augmentation of T-Cell activation by oscillatory forces and engineered antigen-presenting cells. *Nano Lett* 2019;**19**: 6945−54.
14. Champion JA, Mitragotri S. Role of target geometry in phagocytosis. *Proc Natl Acad Sci U S A* 2006;**103**:4930−4.
15. Miao YQ, Yang YT, Guo LM, Chen MS, Zhou X, Zhao YG, et al. Cell membrane-camouflaged nanocarriers with biomimetic deformability of erythrocytes for ultralong circulation and enhanced cancer therapy. *ACS Nano* 2022;**16**:6527−40.
16. Nie D, Liu C, Yu MR, Jiang XH, Wang N, Gan Y. Elasticity regulates nanomaterial transport as delivery vehicles: design, characterization, mechanisms and state of the art. *Biomaterials* 2022;**291**:121879.
17. Gan Y. Atomic and subnanometer resolution in ambient conditions by atomic force microscopy. *Surf Sci Rep* 2009;**64**:99−121.
18. Ferry JD. *Viscoelastic properties of polymers*. 3rd ed. New York: Wiley; 1980.
19. Steinkühler J, Fonda P, Bhatia T, Zhao Z, Leomil FSC, Lipowsky R, et al. Superelasticity of plasma- and synthetic membranes resulting from coupling of membrane asymmetry, curvature, and lipid sorting. *Adv Sci (Weinh)* 2021;**8**:2102109.
20. Zhang GL, Xue HY, Sun DZ, Yang SY, Tu M, Zeng R. Soft apoptotic-cell-inspired nanoparticles persistently bind to macrophage

membranes and promote anti-inflammatory and pro-healing effects. *Acta Biomater* 2021;**131**:452−63.
21. Yi X, Gao HJ. Kinetics of receptor-mediated endocytosis of elastic nanoparticles. *Nanoscale* 2017;**9**:454−63.
22. Sun DZ, Zhang GL, Xie MY, Wang YN, Liang XC, Tu M, et al. Softness enhanced macrophage-mediated therapy of inhaled apoptotic-cell-inspired nanosystems for acute lung injury. *J Nanobiotech* 2023;**21**:172.
23. Zhang J, Fu CS, Tian T, Batur S, Lv JY, Xie Q, et al. *In situ* ultrafast self-gelling coacervate powder with antibacterial, antioxidant, and robust wet adhesion properties for hemostasis and wound healing. *Adv Funct Mater* 2025;**35**:2502577.
24. Trotta M, Peira E, Carlotti ME, Gallarate M. Deformable liposomes for dermal administration of methotrexate. *Int J Pharm* 2004;**270**: 119−25.
25. Guillot AJ, Martínez-Navarrete M, Garrigues TM, Melero A. Skin drug delivery using lipid vesicles: a starting guideline for their development. *J Control Release* 2023;**355**:624−54.
26. Cho NJ, Hwang LY, Solandt JJR, Frank CW. Comparison of extruded and sonicated vesicles for planar bilayer self-assembly. *Materials* 2013;**6**:3294−308.
27. Yu SH, Chen WK, Liu GQ, Flores B, DeWolf EL, Fan BW, et al. Glucose-driven droplet formation in complexes of a supramolecular peptide and therapeutic protein. *J Am Chem Soc* 2024;**146**: 7498−505.
28. Hu Q, Lan HB, Tian Y, Li XN, Wang MM, Zhang J, et al. Biofunctional coacervate-based artificial protocells with membrane-like and cytoplasm-like structures for the treatment of persistent hyperuricemia. *J Control Release* 2024;**365**:176−92.
29. Garcia R. Nanomechanical mapping of soft materials with the atomic force microscope: methods, theory and applications. *Chem Soc Rev* 2020;**49**:5850−84.
30. Ge ZX, Dai SC, Yu HB, Zhao JH, Yang WG, Tan WJ, et al. Nanomechanical analysis of living small extracellular vesicles to identify gastric cancer cell malignancy based on a biomimetic peritoneum. *ACS Nano* 2024;**18**:6130−46.
31. Camarero-Espinosa S, Moroni L. Janus 3D printed dynamic scaffolds for nanovibration-driven bone regeneration. *Nat Commun* 2021;**12**: 1031.
32. Meekel JP, Mattei G, Costache VS, Balm R, Blankensteijn JD, Yeung KK. A multilayer micromechanical elastic modulus measuring method in *ex vivo* human aneurysmal abdominal aortas. *Acta Biomater* 2019;**96**:345−53.
33. Shi W, Hass B, Kuss MA, Zhang H, Ryu S, Zhang D, et al. Fabrication of versatile dynamic hyaluronic acid-based hydrogels. *Carbohydr Polym* 2020;**233**:115803.
34. Laurano R, Boffito M, Abrami M, Grassi M, Zoso A, Chiono V, et al. Dual stimuli-responsive polyurethane-based hydrogels as smart drug delivery carriers for the advanced treatment of chronic skin wounds. *Bioact Mater* 2021;**6**:3013−24.
35. Bhattacharjee S. DLS and zeta potential—What they are and what they are not?. *J Control Release* 2016;**235**:337−51.
36. Raza K, Singh B, Mahajan A, Negi P, Bhatia A, Katare OP. Design and evaluation of flexible membrane vesicles (FMVs) for enhanced topical delivery of capsaicin. *J Drug Target* 2010;**19**:293−302.
37. Montazerian H, Davoodi E, Baidya A, Badv M, Haghniaz R, Dalili A, et al. Bio-macromolecular design roadmap towards tough bioadhesives. *Chem Soc Rev* 2022;**51**:9127−73.
38. Ren H, Zhang Z, Cheng XL, Zou Z, Chen XS, He CL. Injectable, self-healing hydrogel adhesives with firm tissue adhesion and on-demand biodegradation for sutureless wound closure. *Sci Adv* 2023;**9**. eadh4327.
39. Zhang XY, Liang YP, Huang SF, Guo BL. Chitosan-based self-healing hydrogel dressing for wound healing. *Adv Colloid Interface Sci* 2024;**332**:103267.
40. Zhang W, Wang RX, Sun ZM, Zhu XW, Zhao Q, Zhang TF, et al. Catechol-functionalized hydrogels: biomimetic design, adhesion mechanism, and biomedical applications. *Chem Soc Rev* 2020;**49**: 433−64.
41. Hou Y, Li YZ, Li YQ, Li D, Guo TL, Deng X, et al. Tuning water-resistant networks in mussel-inspired hydrogels for robust wet tissue and bioelectronic adhesion. *ACS Nano* 2023;**17**:2745−60.
42. Bal-Ozturk A, Cecen B, Avci-Adali M, Topkaya SN, Alarcin E, Yasayan G, et al. Tissue adhesives: from research to clinical translation. *Nano Today* 2021;**36**:101049.
43. Geng HM, Zhang PY, Peng QY, Cui JW, Hao JC, Zeng HB. Principles of cation−π interactions for engineering mussel-inspiredfunctional materials. *Acc Chem Res* 2022;**55**:1171−82.
44. Cintron-Cruz JA, Freedman BR, Lee M, Johnson C, Ijaz H, Mooney DJ. Rapid ultratough topological tissue adhesives. *Adv Mater* 2022;**34**:2205567.
45. Niu XL, Xiao SZ, Huang RY, Huang D, Aifantis KE, Yu H, et al. ZIF-8-modified hydrogel sequentially delivers angiogenic and osteogenic growth factors to accelerate vascularized bone regeneration. *J Control Release* 2024;**374**:154−70.
46. Ma ZW, Bourquard C, Gao QM, Jiang SB, De Iure-Grimmel T, Huo R, et al. Controlled tough bioadhesion mediated by ultrasound. *Science* 2022;**377**:751−5.
47. Nezhad-Mokhtari P, Hasany M, Kohestanian M, Dolatshahi-Pirouz A, Milani M, Mehrali M. Recent advancements in bioadhesive self-healing hydrogels for effective chronic wound care. *Adv Colloid Interface Sci* 2024;**334**:103306.
48. Zhou L, Xi YW, Xue YM, Wang M, Liu YL, Guo Y, et al. Injectable self-healing antibacterial bioactive polypeptide-based hybrid nanosystems for efficiently treating multidrug resistant infection, skin-tumor therapy, and enhancing wound healing. *Adv Funct Mater* 2019;**29**:1806883.
49. Chen YJ, Wang QQ, Li DW, Mensah A, Qiu YY, Ke HZ, et al. Mussel-inspired double cross-linked hydrogels with desirable mechanical properties, strong tissue-adhesiveness, self-healing properties and antibacterial properties. *Mater Sci Eng C Mater Biol Appl* 2021;**120**:111690.
50. Xu JP, Hsu SH. Self-healing hydrogel as an injectable implant: translation in brain diseases. *J Biomed Sci* 2023;**30**:43.
51. Li X, Wang YL, Tian YH, Wang ZG, Zhang LL, Ma JX. Aqueous $AlCl_3$/$ZnCl_2$ solution room-induced the self-growing strategy of expanded topological network for cellulose/polyacrylamide-based solid-state electrolytes. *J Colloid Interface Sci* 2024;**670**:311−22.
52. Xia YL, Zhou XZ, Wang ZZ, Zhang LZ, Xiong XH, Cui YB, et al. Muscle-inspired self-growing anisotropic hydrogels with mechanical training-promoting mechanical properties. *Adv Mater* 2025;**37**: e2416744.
53. Zheng ZM, Chen XM, Wang YF, Wen P, Duan QF, Zhang P, et al. Self-growing hydrogel bioadhesives for chronic wound management. *Adv Mater* 2024;**36**:e2408538.
54. Liang YP, Li M, Yang YT, Qiao LP, Xu HR, Guo BL. pH/Glucose dual responsive metformin release hydrogel dressings with adhesion and self-healing *via* dual-dynamic bonding for athletic diabetic foot wound healing. *ACS Nano* 2022;**16**:3194−207.
55. Sun Q, Hou Y, Chu ZQ, Wei Q. Soft overcomes the hard: flexible materials adapt to cell adhesion to promote cell mechanotransduction. *Bioact Mater* 2022;**10**:397−404.
56. Tian YM, Hu Q, Sun ZJ, Yu YL, Li XN, Tian TY, et al. Colon targeting pH-responsive coacervate microdroplets for treatment of ulcerative colitis. *Small* 2024;**20**:e2311890.
57. Zhao PC, Xia XF, Xu XY, Leung KKC, Rai A, Deng YR, et al. Nanoparticle-assembled bioadhesive coacervate coating with prolonged gastrointestinal retention for inflammatory bowel disease therapy. *Nat Commun* 2021;**12**:7162.
58. Zhao PC, Guo JX, Jiang TS, Xu XY, Chen SR, Li Z, et al. Vacuolated coacervate mediates the bimodal release kinetics of diverse macromolecular drugs *in vivo*. *Mater Today* 2023;**66**:26−35.
59. Anselmo AC, Zhang M, Kumar S, Vogus DR, Menegatti S, Helgeson ME, et al. Elasticity of nanoparticles influences their blood

circulation, phagocytosis, endocytosis, and targeting. *ACS Nano* 2015;**9**:3169−77.
60. Herant M, Heinrich V, Dembo M. Mechanics of neutrophil phagocytosis: behavior of the cortical tension. *J Cell Sci* 2005;**118**: 1789−97.
61. Li MY, Jin XY, Liu T, Fan F, Gao F, Chai S, et al. Nanoparticle elasticity affects systemic circulation lifetime by modulating adsorption of apolipoprotein A−I in corona formation. *Nat Commun* 2022;**13**:4137.
62. Dai Z, Yu MR, Yi X, Wu ZM, Tian FL, Miao YQ, et al. Chain-length- and saturation-tuned mechanics of fluid nanovesicles direct tumor delivery. *ACS Nano* 2019;**13**:7676−89.
63. Yu MR, Song WY, Tian FL, Dai Z, Zhu QL, Ahmad E, et al. Temperature- and rigidity-mediated rapid transport of lipid nanovesicles in hydrogels. *Proc Natl Acad Sci U S A* 2019;**116**:5362−9.
64. Nia HT, Munn LL, Jain RK. Physical traits of cancer. *Science* 2020; **370**:eaaz0868.
65. Morad G, Carman CV, Hagedorn EJ, Perlin JR, Zon LI, Mustafaoglu N, et al. Tumor-derived extracellular vesicles breach the intact blood−brain barrier *via* transcytosis. *ACS Nano* 2019;**13**: 13853−65.
66. Chen SQ, Zhong Y, Fan WF, Xiang JJ, Wang GW, Zhou Q, et al. Enhanced tumour penetration and prolonged circulation in blood of polyzwitterion−drug conjugates with cell-membrane affinity. *Nat Biomed Eng* 2021;**5**:1019−37.
67. Zheng YX, Luo SQ, Xu M, He Q, Xie J, Wu JW, et al. Transepithelial transport of nanoparticles in oral drug delivery: from the perspective of surface and holistic property modulation. *Acta Pharm Sin B* 2024;**14**:3876−900.
68. Gadalla HH, Yuan ZY, Chen Z, Alsuwayyid F, Das S, Mitra H, et al. Effects of nanoparticle deformability on multiscale biotransport. *Adv Drug Deliv Rev* 2024;**213**:115445.
69. Zhang MM, Gao S, Yang DJ, Fang Y, Lin XJ, Jin XC, et al. Influencing factors and strategies of enhancing nanoparticles into tumors *in vivo*. *Acta Pharm Sin B* 2021;**11**:2265−85.
70. Yu MR, Xu L, Tian FL, Su Q, Zheng N, Yang YW, et al. Rapid transport of deformation-tuned nanoparticles across biological hydrogels and cellular barriers. *Nat Commun* 2018;**9**:2607.
71. Li Z, Zhu YB, Zhang ZJ, Wang HM, Wang C, Xu C, et al. Softness-aided mild hyperthermia boosts stiff nanomedicine by regulating tumor mechanics. *Adv Sci (Weinh)* 2024;**11**:e2306730.
72. Tao J, Tian Y, Chen D, Lu W, Chen K, Xu C, et al. Stiffness-transformable nanoplatforms responsive to the tumor microenvironment for enhanced tumor therapeutic efficacy. *Angew Chem Int Ed Engl* 2023;**62**:e202216361.
73. Mazumdar S, Chitkara D, Mittal A. Exploration and insights into the cellular internalization and intracellular fate of amphiphilic polymeric nanocarriers. *Acta Pharm Sin B* 2021;**11**:903−24.
74. Yuan PF, Yan XD, Zong XQ, Li XD, Yang CQ, Chen XJ, et al. Modulating elasticity of liposome for enhanced cancer immunotherapy. *ACS Nano* 2024;**18**:23797−811.
75. Li Z, Zhu Y, Zeng H, Wang C, Xu C, Wang Q, et al. Mechano-boosting nanomedicine antitumour efficacy by blocking the reticuloendothelial system with stiff nanogels. *Nat Commun* 2023;**14**: 1437.
76. Shen ZQ, Ye HL, Li Y. Understanding receptor-mediated endocytosis of elastic nanoparticles through coarse grained molecular dynamic simulation. *Phys Chem Chem Phys* 2018;**20**:16372−85.
77. Sun Y, Lau SY, Lim ZW, Chang SC, Ghadessy F, Partridge A, et al. Phase-separating peptides for direct cytosolic delivery and redox-activated release of macromolecular therapeutics. *Nat Chem* 2022; **14**:274−83.
78. Tu ZX, Zhong YL, Hu HZ, Shao D, Haag R, Schirner M, et al. Design of therapeutic biomaterials to control inflammation. *Nat Rev Mater* 2022;**7**:557−74.
79. Jain S, Pitoc GA, Holl EK, Zhang Y, Borst L, Leong KW, et al. Nucleic acid scavengers inhibit thrombosis without increasing bleeding. *Proc Natl Acad Sci U S A* 2012;**109**:12938−43.
80. Schmidt NW, Jin F, Lande R, Curk T, Xian W, Lee C, et al. Liquid-crystalline ordering of antimicrobial peptide−DNA complexes controls TLR9 activation. *Nat Mater* 2015;**14**:696−700.
81. Liu XL, Chen S, Huang J, Du YB, Luo Z, Zhang Y, et al. Synthetic polypeptides inhibit nucleic acid-induced inflammation in autoimmune diseases by disrupting multivalent TLR9 binding to LL37−DNA bundles. *Nat Nanotechnol* 2024;**19**:1745−56.
82. Meng KP, Majedi FS, Thauland TJ, Butte MJ. Mechanosensing through YAP controls T cell activation and metabolism. *J Exp Med* 2020;**217**:e20200053.
83. Atcha H, Jairaman A, Holt JR, Meli VS, Nagalla RR, Veerasubramanian PK, et al. Mechanically activated ion channel Piezo1 modulates macrophage polarization and stiffness sensing. *Nat Commun* 2021;**12**:3256.
84. Meizlish ML, Kimura Y, Pope SD, Matta R, Kim C, Philip NH, et al. Mechanosensing regulates tissue repair program in macrophages. *Sci Adv* 2024;**10**:eadk6906.
85. Chakraborty M, Chu K, Shrestha A, Revelo XS, Zhang X, Gold MJ, et al. Mechanical stiffness controls dendritic cell metabolism and function. *Cell Rep* 2021;**34**:108609.
86. Duan M, Jia Y, Huo L, Gao Y, Wang J, Zhang W, et al. Potentiation of PIEZO2 mechanically-activated currents in sensory neurons mediates vincristine-induced mechanical hypersensitivity. *Acta Pharm Sin B* 2023;**13**:3365−81.
87. Yu H, Liu Z, Guo HX, Hu XY, Wang YY, Cheng XJ, et al. Mechanoimmune-driven backpack sustains dendritic cell maturation for synergistic tumor radiotherapy. *ACS Nano* 2024;**18**:23741−56.
88. Yang ZC, Zhao YG, Zhang XY, Huang L, Wang K, Sun JY, et al. Nano-mechanical immunoengineering: nanoparticle elasticity reprograms tumor-associated macrophages *via* Piezo1. *ACS Nano* 2024;**18**:21221−35.
89. Drobot B, Iglesias-Artola JM, Le Vay K, Mayr V, Kar M, Kreysing M, et al. Compartmentalised RNA catalysis in membrane-free coacervate protocells. *Nat Commun* 2018;**9**:3643.
90. Poudyal RR, Guth-Metzler RM, Veenis AJ, Frankel EA, Keating CD, Bevilacqua PC. Template-directed RNA polymerization and enhanced ribozyme catalysis inside membraneless compartments formed by coacervates. *Nat Commun* 2019;**10**:490.
91. Xie Q, Chen W, Huang ZJ, Gao Y, Zhang HY, Zhou ZH, et al. Polyphenol-based coacervate droplets as building blocks for protocells and prototissues. *Chem Eng J* 2025;**520**:165905.
92. Chen MJ, Lei K, Guo PS, Liu X, Zhao PC, Han M, et al. Highly stretchable, self-healing, self-adhesive and conductive nanocomposite hydrogels based on multi-reversible interactions as multifunctional strain sensors. *Eur Polym J* 2023;**199**:112482.
93. Deng XX, Huang BX, Wang QH, Wu WL, Coates P, Sefat F, et al. A mussel-inspired antibacterial hydrogel with high cell affinity, toughness, self-healing, and recycling properties for wound healing. *ACS Sustainable Chem Eng* 2021;**9**:3070−82.
94. Zhao NY, Yuan WZ. Functionally integrated bioglass microspheres-composited double-network hydrogel with good tissue adhesion and electrical conductivity for efficient wound treatment and health detection. *Compos Part B-Eng* 2022;**242**:110095.
95. Liu XX, Zhou SJ, Cai BY, Wang YN, Deng D, Wang XL. An injectable and self-healing hydrogel with antibacterial and angiogenic properties for diabetic wound healing. *Biomater Sci* 2022;**10**: 3480−92.
96. Li J, Yu F, Chen G, Liu J, Li XL, Cheng B, et al. Moist-retaining, self-recoverable, boadhesive, and transparent *in situ* forming hydrogels to accelerate wound healing. *ACS Appl Mater Interfaces* 2020; **12**:2023−38.
97. Yang R, Liu X, Ren YH, Xue WL, Liu S, Wang PH, et al. Injectable adaptive self-healing hyaluronic acid/poly (γ-glutamic acid) hydrogel for cutaneous wound healing. *Acta Biomater* 2021;**127**:102−15.
98. Nie L, Wei QQ, Sun M, Ding P, Wang L, Sun YF, et al. Injectable, self-healing, transparent, and antibacterial hydrogels based on chitosan and dextran for wound dressings. *Int J Biol Macromol* 2023; **233**:123494.

99. Li SD, Chen N, Li XP, Li Y, Xie ZP, Ma ZY, et al. Bioinspired double-dynamic-bond crosslinked bioadhesive enables post-wound closure care. *Adv Funct Mater* 2020;**30**:2000130.
100. Zhao X, Liang YP, Huang Y, He JH, Han Y, Guo BL. Physical double-network hydrogel adhesives with rapid shape adaptability, fast self-healing, antioxidant and NIR/pH stimulus-responsiveness for multidrug-resistant bacterial infection and removable wound dressing. *Adv Funct Mater* 2020;**30**:1910748.
101. Sun FF, Bu YZ, Chen YR, Yang F, Yu JK, Wu DC. An injectable and instant self-healing medical adhesive for wound sealing. *ACS Appl Mater Interfaces* 2020;**12**:9132−40.
102. Yang ZF, Huang RK, Zheng BN, Guo WT, Li CK, He WY, et al. Highly stretchable, adhesive, biocompatible, and antibacterial hydrogel dressings for wound healing. *Adv Sci (Weinh)* 2021;**8**: 2003627.
103. Liang Y, Li M, Yang Y, Qiao L, Xu H, Guo B. pH/glucose dual responsive metformin release hydrogel dressings with adhesion and self-healing *via* dual-dynamic bonding for athletic diabetic foot wound healing. *ACS Nano* 2022;**16**:3194−207.
104. Deng PP, Liang X, Chen FX, Chen Y, Zhou JP. Novel multifunctional dual-dynamic-bonds crosslinked hydrogels for multi-strategy therapy of MRSA-infected wounds. *Appl Mater Today* 2022; **26**:101362.
105. Zhu Y, Lin L, Xie YT, Wang QH, Gu CH, Chen Y, et al. *In situ* self-assembly of polydopamine inside injectable hydrogels: antibacterial activity and photothermal therapy for superbug-infected wound healing. *Biomater Sci* 2022;**10**:4126−39.
106. Zhang SM, Ding F, Liu Y, Ren XH. Glucose-responsive biomimetic nanoreactor in bacterial cellulose hydrogel for antibacterial and hemostatic therapies. *Carbohydr Polym* 2022;**292**: 119615.
107. Lv ZH, Hu TT, Bian YX, Wang GY, Wu ZK, Li H, et al. A MgFe-LDH nanosheet-incorporated smart thermo-responsive hydrogel with controllable growth factor releasing capability for bone regeneration. *Adv Mater* 2023;**35**:e2206545.
108. Xia Y, Wu J, Wei W, Du Y, Wan T, Ma X, et al. Exploiting the pliability and lateral mobility of Pickering emulsion for enhanced vaccination. *Nat Mater* 2018;**17**:187−94.
109. Guo ZF, Wu FH, Guo CQ, Hu R, Ou YS, Zhu YN, et al. Metal-loparticle-engineered pickering emulsion displaying AAV-Vectored vaccine for enhancing antigen expression and immunogenicity against pathogens. *Adv Mater* 2025;**37**:e2412627.
110. Meng WH, Sun HN, Mu TH, Garcia-Vaquero M. Chitosan-based Pickering emulsion: a comprehensive review on their stabilizers, bioavailability, applications and regulations. *Carbohydr Polym* 2023; **304**:120491.
111. Han J, Chen FL, Gao CC, Zhang Y, Tang XZ. Environmental stability and curcumin release properties of Pickering emulsion stabilized by chitosan/gum arabic nanoparticles. *Int J Biol Macromol* 2020;**157**: 202−11.
112. Cai L, Cao M, Regenstein J. Slow-release and nontoxic pickering emulsion platform for antimicrobial peptide. *J Agric Food Chem* 2020;**68**:7453−66.
113. Peng S, Cao FQ, Xia YF, Gao XD, Dai LP, Yan JH, et al. Particulate alum *via* pckering emulsion for an enhanced COVID-19 vaccine adjuvant. *Adv Mater* 2020;**32**:e2004210.
114. Wu SH, Zhou Y, Asakawa N, Wen M, Sun Y, Ming YL, et al. Engineering CaP-Pickering emulsion for enhanced mRNA cancer vaccines *via* dual DC and NK activations. *J Control Release* 2024;**373**: 837−52.
115. Tselikas L, de Baere T, Isoardo T, Susini S, Ser-Le Roux K, Polrot M, et al. Pickering emulsions with ethiodized oil and nanoparticles for slow release of intratumoral anti-CTLA4 immune checkpoint antibodies. *J Immunother Cancer* 2020;**8**:e000579.
116. Song TT, Xia YF, Du YQ, Chen MW, Qing H, Ma GH. Engineering the deformability of albumin-stabilized emulsions for lymph-node vaccine delivery. *Adv Mater* 2021;**33**:e2100106.
117. Pinot M, Vanni S, Pagnotta S, Lacas-Gervais S, Payet LA, Ferreira T, et al. Polyunsaturated phospholipids facilitate membrane deformation and fission by endocytic proteins. *Science* 2014;**345**:693−7.
118. Guo P, Liu DX, Subramanyam K, Wang BR, Yang J, Huang J, et al. Nanoparticle elasticity directs tumor uptake. *Nat Commun* 2018;**9**: 130.
119. Touitou E, Dayan N, Bergelson L, Godin B, Eliaz M. Ethosomes−novel vesicular carriers for enhanced delivery: characterization and skin penetration properties. *J Control Release* 2000;**65**:403−18.
120. Manca ML, Zaru M, Manconi M, Lai F, Valenti D, Sinico C, et al. Glycerosomes: a new tool for effective dermal and transdermal drug delivery. *Int J Pharm* 2013;**455**:66−74.
121. Manca ML, Manconi M, Zaru M, Valenti D, Peris JE, Matricardi P, et al. Glycerosomes: investigation of role of 1,2-dimyristoyl-*sn*-glycero-3-phosphatidycholine (DMPC) on the assembling and skin delivery performances. *Int J Pharm* 2017;**532**:401−7.
122. Chen JY, Agrawal S, Yi HP, Vallejo D, Agrawal A, Lee AP. Cell-sized lipid vesicles as artificial antigen-presenting cells for antigen-specific T cell activation. *Adv Healthcare Mater* 2023;**12**:e2203163.
123. Song CK, Balakrishnan P, Shim CK, Chung SJ, Chong S, Kim DD. A novel vesicular carrier, transethosome, for enhanced skin delivery of voriconazole: characterization and *in vitro/in vivo* evaluation. *Colloids Surf B Biointerfaces* 2012;**92**:299−304.
124. Hassan AS, Hofni A, Abourehab MAS, Abdel-Rahman IAM. Ginger extract-loaded transethosomes for effective transdermal permeation and anti-inflammation in rat model. *Int J Nanomed* 2023;**18**: 1259−80.
125. Liang QL, Bie NN, Yong TY, Tang K, Shi XL, Wei ZH, et al. The softness of tumour-cell-derived microparticles regulates their drug-delivery efficiency. *Nat Biomed Eng* 2019;**3**:729−40.
126. Shang LH, Xie Q, Yang CL, Kong L, Zhang ZP. Extracellular vesicles facilitate the transportation of nanoparticles within and between cells for enhanced tumor therapy. *ACS Appl Mater Interfaces* 2023; **15**:42378−94.
127. Zhuo Y, Luo Z, Zhu Z, Wang J, Li X, Zhang Z, et al. Direct cytosolic delivery of siRNA *via* cell membrane fusion using cholesterol-enriched exosomes. *Nat Nanotechnol* 2024;**19**:1858−68.
128. Abbas M, Lipinski WP, Wang J, Spruijt E. Peptide-based coacervates as biomimetic protocells. *Chem Soc Rev* 2021;**50**:3690−705.
129. Modderman RST, Holleman LWJ. Coacervation. *Nature* 1932;**129**: 654.
130. Sabari BR, Dall'Agnese A, Boija A, Klein IA, Coffey EL, Shrinivas K, et al. Coactivator condensation at super-enhancers links phase separation and gene control. *Science* 2018;**361**:eaar3958.
131. Du M, Chen ZJ. DNA-induced liquid phase condensation of cGAS activates innate immune signaling. *Science* 2018;**361**:704−9.
132. Pessina F, Giavazzi F, Yin YD, Gioia U, Vitelli V, Galbiati A, et al. Functional transcription promoters at DNA double-strand breaks mediate RNA-driven phase separation of damage-response factors. *Nat Cell Biol* 2019;**21**:1286−99.
133. Liu JH, Spruijt E, Miserez A, Langer R. Peptide-based liquid droplets as emerging delivery vehicles. *Nat Rev Mater* 2023;**8**:139−41.
134. Calhoun MA, Bentil SA, Elliott E, Otero JJ, Winter JO, Dupaix RB. Beyond linear elastic modulus: viscoelastic models for brain and brain mimetic hydrogels. *ACS Biomater Sci Eng* 2019;**5**:3964−73.
135. Liao ZT, Jia BW, Guan DS, Chen XD, Zhang MJ, Tong P. Emergent mechanics of a networked multivalent protein condensate. *Nat Commun* 2025;**16**:5237.
136. Klein IA, Boija A, Afeyan LK, Hawken SW, Fan M, Dall'Agnese A, et al. Partitioning of cancer therapeutics in nuclear condensates. *Science* 2020;**368**:1386−92.
137. Forenzo C, Larsen J. Complex coacervates as a promising vehicle for mRNA delivery: a comprehensive review of recent advances and challenges. *Mol Pharm* 2023;**20**:4387−403.
138. Ban E, Kim A. Coacervates: recent developments as nanostructure delivery platforms for therapeutic biomolecules. *Int J Pharm* 2022; **624**:122058.

139. Shebanova A, Perrin QM, Zhu KX, Gudlur S, Chen ZL, Sun Y, et al. Cellular uptake of phase-separating peptide coacervates. *Adv Sci (Weinh)* 2024;**11**:e2402652.
140. Chen WX, Dúzs B, Argudo PG, Bauer SV, Liu W, Samanta A, et al. Ballistic diffusion fronts in biomolecular condensates. *Nat Nanotechnol* 2025;**20**:1062−70.
141. Cao S, Ivanov T, Heuer J, Ferguson CTJ, Landfester K, Caire da Silva L. Dipeptide coacervates as artificial membraneless organelles for bioorthogonal catalysis. *Nat Commun* 2024;**15**:39.
142. Xu C, Martin N, Li M, Mann S. Living material assembly of bacteriogenic protocells. *Nature* 2022;**609**:1029−37.
143. Xie X, Li TJ, Ma LJ, Wu JH, Qi YJ, Yang BG, et al. A designer minimalistic model parallels the phase-separation-mediated assembly and biophysical cues of extracellular matrix. *Nat Chem* 2025;**17**: 1216−26.
144. Li X, Nakagawa S, Tsuji Y, Watanabe N, Shibayama M. Polymer gel with a flexible and highly ordered three-dimensional network synthesized *via* bond percolation. *Sci Adv* 2019;**5**:eaax8647.
145. Sun HL, Han YP, Huang MJ, Li JW, Bian ZY, Wang YL, et al. Highly stretchable, environmentally stable, self-healing and adhesive conductive nanocomposite organohydrogel for efficient multimodal sensing. *Chem Eng J* 2024;**480**:148305.
146. Wang LR, Xu TL, Zhang XJ. Multifunctional conductive hydrogel-based flexible wearable sensors. *TrAC, Trends Anal Chem* 2021; **134**:116130.
147. Xu CG, Chen Y, Zhao SY, Li DK, Tang X, Zhang HL, et al. Mechanical regulation of polymer gels. *Chem Rev* 2024;**124**: 10435−508.
148. Zou CY, Lei XX, Hu JJ, Jiang YL, Li QJ, Song YT, et al. Multi-crosslinking hydrogels with robust bio-adhesion and pro-coagulant activity for first-aid hemostasis and infected wound healing. *Bioact Mater* 2022;**16**:388−402.
149. Tran HN, Kim IG, Kim JH, Chung EJ, Noh I. Control of maleic acid-propylene diepoxide hydrogel for 3D printing application for flexible tissue engineering scaffold with high resolution by end capping and graft polymerization. *Biomater Res* 2022;**26**:75.
150. Li GJ, Zhao ZH, Zhang SL, Sun L, Li MN, Yuwono JA, et al. A biocompatible electrolyte enables highly reversible Zn anode for zinc ion battery. *Nat Commun* 2023;**14**:6526.
151. Wang L, Ding XY, Fan L, Filppula AM, Li QY, Zhang HB, et al. Self-healing dynamic hydrogel microparticles with structural color for wound management. *Nano-Micro Lett* 2024;**16**:232.
152. Chen Y, Wang X, Tao S, Wang Q, Ma PQ, Li ZB, et al. Research advances in smart responsive-hydrogel dressings with potential clinical diabetic wound healing properties. *Mil Med Res* 2023;**10**:37.
153. Xie QQ, Yan CC, Liu GH, Bian LM, Zhang KY. *In situ* triggered self-contraction bioactive microgel assembly accelerates diabetic skin wound healing by activating mechanotransduction and biochemical pathway. *Adv Mater* 2024;**36**:2406434.
154. Bertsch P, Diba M, Mooney DJ, Leeuwenburgh SCG. Self-healing injectable hydrogels for tissue regeneration. *Chem Rev* 2023;**123**: 834−73.
155. Tang HH, Yang YY, Liu Z, Li WL, Zhang YP, Huang YZ, et al. Injectable ultrasonic sensor for wireless monitoring of intracranial signals. *Nature* 2024;**630**:84−90.
156. Wang XJ, Hao XR, Zhang YN, Wu Q, Zhou JJ, Cheng ZM, et al. Bioinspired adaptive microdrugs enhance the chemotherapy of malignant glioma: beyond their nanodrugs. *Adv Mater* 2024;**36**: e2405165.
157. Liu JQ, Liu N, Xu Y, Wu M, Zhang H, Wang Y, et al. Bioresorbable shape-adaptive structures for ultrasonic monitoring of deep-tissue homeostasis. *Science* 2024;**383**:1096−103.
158. Cheng JL, Chen ZY, Lin DM, Yang YF, Bai YJ, Wang LS, et al. A high clinically translatable strategy to anti-aging using hyaluronic acid and silk fibroin co-crosslinked hydrogels as dermal regenerative fillers. *Acta Pharm Sin B* 2025;**15**:3767−87.
159. Askari E, Shokrollahi Barough M, Rahmanian M, Mojtabavi N, Sarrami Forooshani R, Seyfoori A, et al. Cancer immunotherapy using bioengineered micro/nano structured hydrogels. *Adv Healthcare Mater* 2023;**12**:2301174.
160. Duan QY, Zhu YX, Jia HR, Wang SH, Wu FG. Nanogels: synthesis, properties, and recent biomedical applications. *Prog Mater Sci* 2023; **139**:101167.
161. Ho TM, Razzaghi A, Ramachandran A, Mikkonen KS. Emulsion characterization *via* microfluidic devices: a review on interfacial tension and stability to coalescence. *Adv Colloid Interface Sci* 2022; **299**:102541.
162. Keskin D, Zu G, Forson AM, Tromp L, Sjollema J, van Rijn P. Nanogels: a novel approach in antimicrobial delivery systems and antimicrobial coatings. *Bioact Mater* 2021;**6**:3634−57.
163. Sun M, Yue T, Wang CY, Fan Z, Gazit E, Du JZ. Ultrasound-responsive peptide nanogels to balance conflicting requirements for deep tumor penetration and prolonged blood circulation. *ACS Nano* 2022;**16**:9183−94.
164. Bhatia S, Hilsch M, Cuellar-Camacho JL, Ludwig K, Nie C, Parshad B, et al. Adaptive fexible sialylated nanogels as highly potent influenza A virus inhibitors. *Angew Chem Int Ed Engl* 2020; **59**:12417−22.
165. Hu LX, Chee PL, Sugiarto S, Yu Y, Shi CQ, Yan R, et al. Hydrogel-based flexible electronics. *Adv Mater* 2023;**35**:2205326.
166. Correa S, Grosskopf AK, Lopez Hernandez H, Chan D, Yu AC, Stapleton LM, et al. Translational applications of hydrogels. *Chem Rev* 2021;**121**:11385−457.
167. Roy A, Zenker S, Jain S, Afshari R, Oz Y, Zheng YT, et al. A highly stretchable, conductive, and transparent bioadhesive hydrogel as a flexible sensor for enhanced real-time human health monitoring. *Adv Mater* 2024;**36**:e2404225.
168. Cho KW, Sunwoo SH, Hong YJ, Koo JH, Kim JH, Baik S, et al. Soft bioelectronics based on nanomaterials. *Chem Rev* 2022;**122**: 5068−143.
169. Apsite I, Salehi S, Ionov L. Materials for smart soft actuator systems. *Chem Rev* 2022;**122**:1349−415.
170. Lin JS, Chen XM, Zhang P, Xue Y, Feng YH, Ni ZP, et al. Wireless bioelectronics for *in vivo* pressure monitoring with mechanically-compliant hydrogel biointerfaces. *Adv Mater* 2024; **36**:2400181.
171. Zhao B, Bai ZY, Lv HL, Yan ZK, Du YQ, Guo XQ, et al. Self-healing liquid metal magnetic hydrogels for smart feedback sensors and high-performance electromagnetic shielding. *Nano-Micro Lett* 2023;**15**:79.
172. Jiang YW, Trotsyuk AA, Niu SM, Henn D, Chen K, Shih CC, et al. Wireless, closed-loop, smart bandage with integrated sensors and stimulators for advanced wound care and accelerated healing. *Nat Biotechnol* 2023;**41**:652−62.
173. Jeffreys N, Brockman JM, Zhai Y, Ingber DE, Mooney DJ. Mechanical forces amplify TCR mechanotransduction in T cell activation and function. *Appl Phys Rev* 2024;**11**:011304.
174. Livingston NK, Hickey JW, Sim H, Salathe SF, Choy J, Kong JY, et al. *In vivo* stimulation of therapeutic antigen-specific T cells in an artificial lymph node matrix. *Adv Mater* 2024;**36**:2310043.
175. Joseph JP, Gugulothu SB, Nandi D, Chatterjee K. Mechanical properties affect primary T cell activation in 3D bioprinted hydrogels. *ACS Macro Lett* 2023;**12**:1085−93.
176. Weiden J, Voerman D, Dölen Y, Das RK, van Duffelen A, Hammink R, et al. Injectable biomimetic hydrogels as tools for efficient T cell expansion and delivery. *Front Immunol* 2018;**9**:2798.
177. Bhatta R, Han J, Liu YS, Bo Y, Wang H. T cell-responsive macroporous hydrogels for *in situ* T cell expansion and enhanced antitumor efficacy. *Biomaterials* 2023;**293**:121972.
178. Xue TT, Zhang JB, Li FF, Chen GP, Yi K, Chen XD, et al. Tunable biomechanical niches regulate hepatic differentiation of mesenchymal stem cells for acute liver failure therapy. *Biomaterials* 2025; **324**:123458.

179. A N, Kovooru L, Behera AK, Kumar KPP, Srivastava P. A critical review of synthesis procedures, applications and future potential of nanoemulsions. *Adv Colloid Interface Sci* 2021;**287**:102318.
180. He X, Lu QY. A review of high internal phase pickering emulsions: stabilization, rheology, and 3D printing application. *Adv Colloid Interface Sci* 2024;**324**:103086.
181. Xia YF, Na XM, Wu J, Ma GH. The horizon of the emulsion particulate strategy: engineering hollow particles for biomedical applications. *Adv Mater* 2019;**31**:e1801159.
182. Pang B, Liu H, Zhang K. Recent progress on Pickering emulsions stabilized by polysaccharides-based micro/nanoparticles. *Adv Colloid Interface Sci* 2021;**296**:102522.
183. Yang D, Feng YQ, Yao XL, Zhao BF, Li D, Liu N, et al. Recent advances in bioactive nanocrystal-stabilized Pickering emulsions: fabrication, characterization, and biological assessment. *Compr Rev Food Sci Food Saf* 2023;**22**:946−70.
184. Sharkawy A, Rodrigues AE. Plant gums in Pickering emulsions: a review of sources, properties, applications, and future perspectives. *Carbohydr Polym* 2024;**332**:121900.
185. Albert C, Beladjine M, Tsapis N, Fattal E, Agnely F, Huang N. Pickering emulsions: preparation processes, key parameters governing their properties and potential for pharmaceutical applications. *J Control Release* 2019;**309**:302−32.
186. Low LE, Siva SP, Ho YK, Chan ES, Tey BT. Recent advances of characterization techniques for the formation, physical properties and stability of Pickering emulsion. *Adv Colloid Interface Sci* 2020;**277**: 102117.
187. Wu L, Liao Z, Liu M, Yin X, Li X, Wang M, et al. Fabrication of non-spherical pickering emulsion droplets by cyclodextrins mediated molecular self-assembly. *Colloids Surf A Physicochem Eng Asp* 2016;**490**:163−72.
188. Ahuja A, Potanin A, Joshi YM. Two step yielding in soft materials. *Adv Colloid Interface Sci* 2020;**282**:102179.
189. McKenzie TJ, Ayres N. Synthesis and applications of elastomeric polymerized high internal phase emulsions (PolyHIPEs). *ACS Omega* 2023;**8**:20178−95.
190. Xia YF, Wu J, Wei W, Du YQ, Wan T, Ma XW, et al. Exploiting the pliability and lateral mobility of Pickering emulsion for enhanced vaccination. *Nat Mater* 2018;**17**:187−94.
191. Chen QT, Wu N, Gao YH, Wang XJ, Wu J, Ma GH. Alum pickering emulsion as effective adjuvant to improve malaria vaccine efficacy. *Vaccines (Basel)* 2021;**9**:1244.
192. Zou YJ, Liu XX, Chen QT, Oku H, Ma GH, Wu J. Acid-responsive immune-enhancing chitosan formulation capable of transforming from particle stabilization to polymer chain stabilization. *ACS Appl Mater Interfaces* 2023;**15**:11403−15.
193. Wu N, Chen QT, Zou YJ, Miao CY, Ma GH, Wu J. Chitosan particle-emulsion complex adjuvants: the effect of particle distribution on the immune intensity and response type. *Carbohydr Polym* 2023;**309**: 120673.
194. Peng S, Yan YM, Ogino K, Ma GH, Xia YF. Spatiotemporal coordination of antigen presentation and co-stimulatory signal for enhanced anti-tumor vaccination. *J Control Release* 2024;**374**: 312−24.
195. Du YQ, Lv JL, Hao ZW, Li ZF, Song TT, Ge HF, et al. Pickering emulsion-guided monomeric delivery of monophosphoryl lipid A for enhanced vaccination. *J Control Release* 2024;**374**:39−49.
196. Cao FQ, Peng S, An YL, Xu K, Zheng TY, Dai LP, et al. Inside-out assembly of viral antigens for the enhanced vaccination. *Signal Transduct Targeted Ther* 2023;**8**:189.
197. Yang N, Kang YT, Cong YJ, Wang XY, Yao C, Wang S, et al. Controllable gold nanocluster-emulsion interface for direct cell penetration and photothermal killing. *Adv Mater* 2023;**35**:e2208349.
198. Chen JP, Pan JH, Liu SJ, Zhang YN, Sha SN, Guo HY, et al. Fruit-derived extracellular-vesicle-engineered structural droplet drugs for enhanced glioblastoma chemotherapy. *Adv Mater* 2023;**35**:2304187.
199. Wang CJ, Zhang L, Yang ZJ, Zhao DX, Deng Z, Xu JL, et al. Self-fueling ferroptosis-inducing microreactors based on pH-responsive lpiodol pickering emulsions enable transarterial ferro-embolization therapy. *Natl Sci Rev* 2024;**11**:nwad257.
200. Wolf P. The nature and significance of platelet products in human plasma. *Br J Haematol* 1967;**13**:269−88.
201. György B, Szabó TG, Pásztói M, Pál Z, Misják P, Aradi B, et al. Membrane vesicles, current state-of-the-art: emerging role of extracellular vesicles. *Cell Mol Life Sci* 2011;**68**:2667−88.
202. Dixson AC, Dawson TR, Di Vizio D, Weaver AM. Context-specific regulation of extracellular vesicle biogenesis and cargo selection. *Nat Rev Mol Cell Biol* 2023;**24**:454−76.
203. Elsharkasy OM, Nordin JZ, Hagey DW, de Jong OG, Schiffelers RM, Andaloussi SEL, et al. Extracellular vesicles as drug delivery systems: why and how?. *Adv Drug Deliv Rev* 2020;**159**:332−43.
204. Kumar MA, Baba SK, Sadida HQ, Marzooqi SA, Jerobin J, Altemani FH, et al. Extracellular vesicles as tools and targets in therapy for diseases. *Signal Transduct Targeted Ther* 2024;**9**:27.
205. Ye SY, Li WZ, Wang HY, Zhu L, Wang C, Yang YL. Quantitative nanomechanical analysis of small extracellular vesicles for tumor malignancy indication. *Adv Sci (Weinh)* 2021;**8**:e2100825.
206. Ma JW, Zhang Y, Tang K, Zhang HF, Yin XN, Li Y, et al. Reversing drug resistance of soft tumor-repopulating cells by tumor cell-derived chemotherapeutic microparticles. *Cell Res* 2016;**26**:713−27.
207. Guo P, Busatto S, Huang J, Morad G, Moses MA. A facile magnetic extrusion method for preparing endosome-derived vesicles for cancer drug delivery. *Adv Funct Mater* 2021;**31**:2008326.
208. Abu Lila ASIT. Liposomal delivery systems: design optimization and current applications. *Biol Pharm Bull* 2017;**40**:1−10.
209. Tian CA, Chiu CC. Importance of hydrophilic groups on modulating the structural, mechanical, and interfacial properties of bilayers: a comparative molecular dynamics study of phosphatidylcholine and ion pair amphiphile membranes. *Int J Mol Sci* 2018;**19**:1552.
210. Mathiyazhakan M, Wiraja C, Xu CJ. A concise review of gold nanoparticles-based photo-responsive liposomes for controlled drug delivery. *Nano-Micro Lett* 2018;**10**:10.
211. Et-Thakafy O, Delorme N, Guyomarc'h F, Lopez C. Mechanical properties of milk sphingomyelin bilayer membranes in the gel phase: effects of naturally complex heterogeneity, saturation and acyl chain length investigated on liposomes using AFM. *Chem Phys Lipids* 2018;**210**:47−59.
212. Fu XL, Shi YB, Wang H, Zhao XG, Sun QF, Huang Y, et al. Ethosomal gel for improving transdermal delivery of thymosin β-4. *Int J Nanomed* 2019;**14**:9275−84.
213. Sun JS, Zhang L, Wang JL, Feng Q, Liu DB, Yin QF, et al. Tunable rigidity of (polymeric core)-(lipid shell) nanoparticles for regulated cellular uptake. *Adv Mater* 2015;**27**:1402−7.
214. Hu X, Sun Y, Zhou XQ, Zhang B, Guan HX, Xia F, et al. Insight into drug loading regulated micellar rigidity by nuclear magnetic resonance. *ACS Nano* 2022;**16**:21407−16.
215. Tan P, Wu CC, Tang Q, Wang T, Zhou CL, Ding YK, et al. pH-Triggered size-transformable and bioactivity-switchable self-assembling chimeric peptide nanoassemblies for combating drug-resistant bacteria and biofilms. *Adv Mater* 2023;**35**:e2210766.
216. Waeterschoot J, Gosselé W, Lemež Š, Casadevall ISX. Artificial cells for *in vivo* biomedical applications through red blood cell biomimicry. *Nat Commun* 2024;**15**:2504.
217. Nair KS, Bajaj H. Advances in giant unilamellar vesicle preparation techniques and applications. *Adv Colloid Interface Sci* 2023;**318**:102935.
218. de Souza Melchiors M, Ivanov T, Harley I, Sayer C, Araújo PHH, Caire da Silva L, et al. Membrane manipulation of giant unilamellar polymer vesicles with a temperature-responsive polymer. *Angew Chem Int Ed Engl* 2022;**61**:e202207998.
219. Himbert S, Rheinstädter MC. Structural and mechanical properties of the red blood cell's cytoplasmic membrane seen through the lens of biophysics. *Front Physiol* 2022;**13**:953257.
220. Li ST, Meng XR, Peng B, Huang J, Liu JW, Xiao H, et al. Cell membrane-based biomimetic technology for cancer phototherapy: mechanisms, recent advances and perspectives. *Acta Biomater* 2024; **174**:26−48.

221. Sun M, Yang JN, Fan YY, Zhang YF, Sun J, Hu M, et al. Beyond extracellular vesicles: hybrid membrane nanovesicles as emerging advanced tools for biomedical applications. *Adv Sci (Weinh)* 2023;**10**: e2303617.
222. Chiang ST, Chen Q, Han TZ, Qian CX, Shen XS, Lin YJ, et al. Biomimetic nanovesicles synergize with short-term fasting for enhanced chemotherapy of triple-negative breast cancer. *ACS Nano* 2024;**18**:33875−89.
223. Yao WJ, Liu WW, Su FS, Wang JR, Li H, Sun MH, et al. Hybrid membrane-camouflaged biomimetic immunomodulatory nanoturrets with sequential multidrug release for potentiating T cell-mediated anticancer immunity. *J Am Chem Soc* 2024;**146**:18592−605.
224. Glassman PM, Hood ED, Ferguson LT, Zhao Z, Siegel DL, Mitragotri S, et al. Red blood cells: the metamorphosis of a neglected carrier into the natural mothership for artificial nanocarriers. *Adv Drug Deliv Rev* 2021;**178**:113992.
225. Wang HW, Alarcón CN, Liu B, Watson F, Searles S, Lee CK, et al. Genetically engineered and enucleated human mesenchymal stromal cells for the targeted delivery of therapeutics to diseased tissue. *Nat Biomed Eng* 2022;**6**:882−97.
226. Kansız S, Elçin YM. Advanced liposome and polymersome-based drug delivery systems: considerations for physicochemical properties, targeting strategies and stimuli-sensitive approaches. *Adv Colloid Interface Sci* 2023;**317**:102930.
227. Sun QM, Shi JQ, Sun H, Zhu YQ, Du JZ. Membrane and lumen-compartmentalized polymersomes for biocatalysis and cell mimics. *Biomacromolecules* 2023;**24**:4587−604.
228. Wang XL, Liu XM, Huang X. Bioinspired protein-based assembling: toward advanced life-like behaviors. *Adv Mater* 2020; **32**:e2001436.
229. Liu ZT, Liu L, Huang R, Xu FJ, Zhao NN, Lin YY. Engineering protocell networks for prototissue development. *Adv Healthcare Mater* 2025;**14**:e2500376.
230. Tang M, Lin K, Ramachandran M, Li L, Zou H, Zheng H, et al. A mitochondria-targeting lipid-small molecule hybrid nanoparticle for imaging and therapy in an orthotopic glioma model. *Acta Pharm Sin B* 2022;**12**:2672−82.
231. Gaur D, Dubey NC, Tripathi BP. Biocatalytic self-assembled synthetic vesicles and coacervates: from single compartment to artificial cells. *Adv Colloid Interface Sci* 2022;**299**:102566.
232. Li F, Wang DB, Zhou J, Men D, Zhan XE. Design and biosynthesis of functional protein nanostructures. *Sci China Life Sci* 2020;**63**: 1142−58.
233. Theil EC. Ferritin protein nanocages use ion channels, catalytic sites, and nucleation channels to manage iron/oxygen chemistry. *Curr Opin Chem Biol* 2011;**15**:304−11.
234. Jergens E, Winter JO. Nanoparticles caged with DNA nanostructures. *Curr Opin Biotechnol* 2022;**74**:278−84.
235. Wang J, Li Z, Willner I. Dynamic reconfigurable DNA nanostructures, networks and materials. *Angew Chem Int Ed Engl* 2023; **62**:e202215332.
236. Sun Y, Wu X, Shen K, Guo K, Lim DS, Chew WL, et al. Polyethylene-glycol-conjugated peptide coacervates with tunable size for intracellular mRNA delivery. *ACS Nano* 2025;**19**:24724−35.
237. Johnson NR, Wang Y. Coacervate delivery of HB-EGF accelerates healing of type 2 diabetic wounds. *Wound Repair Regen* 2015;**23**: 591−600.
238. Gao XQ, Cheng H, Awada H, Tang Y, Amra S, Lu AP, et al. A comparison of BMP2 delivery by coacervate and gene therapy for promoting human muscle-derived stem cell-mediated articular cartilage repair. *Stem Cell Res Ther* 2019;**10**:346.
239. Souri M, Yim WJ, Halder M, Jin ZC, Jokerst JV. Coacervate-based selivery systems: bridging fundamentals and applications. *ACS Appl Mater Interfaces* 2025;**17**:41513−53.
240. Yuan JW, Yang YF, Dai K, Fakhrullin R, Li H, Zhou P, et al. Peptide coacervates: formation, mechanism, and biological applications. *ACS Appl Mater Interfaces* 2025;**17**:27697−712.
241. Lee J, Pir Cakmak F, Booth R, Keating CD. Hybrid protocells based on coacervate-templated fatty acid vesicles combine improved membrane stability with functional interior protocytoplasm. *Small* 2024;**20**:e2406671.
242. Ngocho K, Yang XL, Wang ZF, Hu CJ, Yang XH, Shi H, et al. Synthetic cells from droplet-based microfluidics for biosensing and biomedical applications. *Small* 2024;**20**:2400086.
243. Huang XY, Zheng C, Ding KL, Zhang SM, Lei Y, Wei QR, et al. Dual-crosslinked bioprosthetic heart valves prepared by glutaraldehyde crosslinked pericardium and poly-2-hydroxyethyl methacrylate exhibited improved antithrombogenicity and anticalcification properties. *Acta Biomater* 2022;**154**:244−58.
244. Iglesias-Mejuto A, García-González CA. 3D-printed alginate-hydroxyapatite aerogel scaffolds for bone tissue engineering. *Mater Sci Eng C* 2021;**131**:112525.
245. Du YQ, Song TT, Wu J, Gao XD, Ma GH, Liu YC, et al. Engineering mannosylated pickering emulsions for the targeted delivery of multicomponent vaccines. *Biomaterials* 2022;**280**:121313.
246. Heidari-Dalfard F, Tavasoli S, Assadpour E, Miller R, Jafari SM. Surface modification of particles/nanoparticles to improve the stability of Pickering emulsions; a critical review. *Adv Colloid Interface Sci* 2025;**336**:103378.
247. Jiang JK, Poortinga AT, Liao YY, Kamperman T, Venner CH, Visser CW. High-throughput fabrication of size-controlled pickering emulsions, colloidosomes, and air-coated particles *via* clog-free jetting of suspensions. *Adv Mater* 2023;**35**:2208894.
248. Niroula A, Poortinga AT, Nazir A. Pickering stabilization of double emulsions: basic concepts, rationale, preparation, potential applications, challenges, and future perspectives. *Adv Colloid Interface Sci* 2025;**343**:103531.
249. Larey AM, Spoerer TM, Daga KR, Morfin MG, Hynds HM, Carpenter J, et al. High throughput screening of mesenchymal stromal cell morphological response to inflammatory signals for bioreactor-based manufacturing of extracellular vesicles that modulate microglia. *Bioact Mater* 2024;**37**:153−71.
250. Kim S, Kim YK, Kim S, Choi YS, Lee I, Joo H, et al. Dual-mode action of scalable, high-quality engineered stem cell-derived SIRPα-extracellular vesicles for treating acute liver failure. *Nat Commun* 2025;**16**:1903.
251. Rai A, Claridge B, Lozano J, Greening DW. The discovery of extracellular vesicles and their emergence as a next-generation therapy. *Circ Res* 2024;**135**:198−221.
252. Richter M, Vader P, Fuhrmann G. Approaches to surface engineering of extracellular vesicles. *Adv Drug Deliv Rev* 2021;**173**:416−26.
253. Kieler-Ferguson HM, Chan D, Sockolosky J, Finney L, Maxey E, Vogt S, et al. Encapsulation, controlled release, and antitumor efficacy of cisplatin delivered in liposomes composed of sterol-modified phospholipids. *Eur J Pharmaceut Sci* 2017;**103**:85−93.
254. White SC, Lorigan P, Margison GP, Margison JM, Martin F, Thatcher N, et al. Phase II study of SPI-77 (sterically stabilised liposomal cisplatin) in advanced non-small-cell lung cancer. *Br J Cancer* 2006;**95**:822−8.
255. Dou YN, Hynynen K, Allen C. To heat or not to heat: challenges with clinical translation of thermosensitive liposomes. *J Control Release* 2017;**249**:63−73.